ASSESSMENT OF WASHINGTON STATE BRIDGES FOR POST-EARTHQUAKE MOBILITY AND RECOVERY PLANNING

FINAL PROJECT REPORT

by

Adam R. Phillips and Christopher J. Motter
Washington State University

Sponsorship
Washington State University

for

Pacific Northwest Transportation Consortium (PacTrans)
USDOT University Transportation Center for Federal Region 10
University of Washington
More Hall 112, Box 352700
Seattle, WA 98195-2700

In cooperation with U.S. Department of Transportation,
Office of the Assistant Secretary for Research and Technology (OST-R)

DISCLAIMER

The contents of this report reflect the views of the authors, who are responsible for the facts and the accuracy of the information presented herein. This document is disseminated under the sponsorship of the U.S. Department of Transportation's University Transportation Centers Program, in the interest of information exchange. The Pacific Northwest Transportation Consortium, the U.S. Government and matching sponsor assume no liability for the contents or use thereof.

TECHNICAL REPORT DOCUMENTATION PAGE

1. Report No.	2. Government Accession No.	3. Recipient's Catalog No.

4. Title and Subtitle	5. Report Date
Assessment of Washington State Bridges for Post-Earthquake Mobility and Recovery Planning	September 2021
	6. Performing Organization Code

7. Author(s) and Affiliations	8. Performing Organization Report No.
Adam R. Phillips, 0000-0003-2486-6039; Christopher J. Motter, 0000-0003-0418-3791; Washington State University	2020-S-WSU-2

9. Performing Organization Name and Address	10. Work Unit No. (TRAIS)
PacTrans Pacific Northwest Transportation Consortium University Transportation Center for Federal Region 10 University of Washington More Hall 112 Seattle, WA 98195-2700	**11. Contract or Grant No.** 69A3551747110

12. Sponsoring Organization Name and Address	13. Type of Report and Period Covered
United States Department of Transportation Research and Innovative Technology Administration 1200 New Jersey Avenue, SE Washington, DC 20590	Final Report, August 2020 – August 2021
	14. Sponsoring Agency Code

15. Supplementary Notes

Report uploaded to: www.pactrans.org

16. Abstract

A 2019 Department of Homeland Security report assessing the regional resiliency of Western Washington state to a Cascadia Subduction Zone earthquake predicted widespread and high levels of bridge damage. Because of this report, the state's emergency response and recovery plan is heavily reliant on air transportation modes to provide resources to the affected populations. However, surface transportation modes, if available, are better suited for moving large volumes of resources and serving as critical lifelines for impacted regions of the state. The goal of this study was to improve the prediction of non-functional, partially functional, and functional bridges to assist in post-earthquake emergency planning. This research project focused on determining the functionality of bridges along the routes that connect to the main WSDOT critical lifeline corridors of I-5/405 and I-90. WSDOT has active research projects that are focusing on the resiliency of the I-5/405/90 lifeline routes but are not directly assessing the functionality of the routes connecting into it. Without these secondary routes, the post-earthquake mobility of the state will be reduced, emergency management plans will be difficult to enact, and long-term recovery will be impaired.

This study used updated bridge models, based on a database of important characteristics of selected bridges across Washington state, and 60 synthetic Cascadia Subduction Zone earthquake ground motions to improve predictions of likely loss of functionality for bridges along the secondary state routes of 101, 12, 16, and 3. Results of these analyses were that very few, if any, bridges are expected to be completely destroyed, resulting in no functionality post-earthquake. Bridges inland of the coast and outside of the sedimentary basins of Seattle, Port Angeles, and Tacoma were predicted to remain fully functional post-earthquake. Lastly, bridges located along the coast are likely to sustain damage requiring repair but should be partially functional within 3 to 6 months post-earthquake, based on estimates from the Washington Bridge Design Manual. These results considered only multi-span bridges supported by piers with reinforced concrete columns. Single-span bridges were omitted but are expected to remain functional. Other bridges would need to be evaluated on a case-by-case basis, and liquefaction was omitted but could cause significant bridge damage.

17. Key Words	18. Distribution Statement
Loss and Damage;	

19. Security Classification (of this report)	20. Security Classification (of this page)	21. No. of Pages	22. Price
Unclassified.	Unclassified.	46	N/A

SI* (MODERN METRIC) CONVERSION FACTORS

APPROXIMATE CONVERSIONS TO SI UNITS

Symbol	When You Know	Multiply By	To Find	Symbol
		LENGTH		
in	inches	25.4	millimeters	mm
ft	feet	0.305	meters	m
yd	yards	0.914	meters	m
mi	miles	1.61	kilometers	km
		AREA		
in^2	square inches	645.2	square millimeters	mm^2
ft^2	square feet	0.093	square meters	m^2
yd^2	square yard	0.836	square meters	m^2
ac	acres	0.405	hectares	ha
mi^2	square miles	2.59	square kilometers	km^2
		VOLUME		
fl oz	fluid ounces	29.57	milliliters	mL
gal	gallons	3.785	liters	L
ft^3	cubic feet	0.028	cubic meters	m^3
yd^3	cubic yards	0.765	cubic meters	m^3
		NOTE: volumes greater than 1000 L shall be shown in m^3		
		MASS		
oz	ounces	28.35	grams	g
lb	pounds	0.454	kilograms	kg
T	short tons (2000 lb)	0.907	megagrams (or "metric ton")	Mg (or "t")
		TEMPERATURE (exact degrees)		
°F	Fahrenheit	5 (F-32)/9 or (F-32)/1.8	Celsius	°C
		ILLUMINATION		
fc	foot-candles	10.76	lux	lx
fl	foot-Lamberts	3.426	$candela/m^2$	cd/m^2
		FORCE and PRESSURE or STRESS		
lbf	poundforce	4.45	newtons	N
lbf/in^2	poundforce per square inch	6.89	kilopascals	kPa

APPROXIMATE CONVERSIONS FROM SI UNITS

Symbol	When You Know	Multiply By	To Find	Symbol
		LENGTH		
mm	millimeters	0.039	inches	in
m	meters	3.28	feet	ft
m	meters	1.09	yards	yd
km	kilometers	0.621	miles	mi
		AREA		
mm^2	square millimeters	0.0016	square inches	in^2
m^2	square meters	10.764	square feet	ft^2
m^2	square meters	1.195	square yards	yd^2
ha	hectares	2.47	acres	ac
km^2	square kilometers	0.386	square miles	mi^2
		VOLUME		
mL	milliliters	0.034	fluid ounces	fl oz
L	liters	0.264	gallons	gal
m^3	cubic meters	35.314	cubic feet	ft^3
m^3	cubic meters	1.307	cubic yards	yd^3
		MASS		
g	grams	0.035	ounces	oz
kg	kilograms	2.202	pounds	lb
Mg (or "t")	megagrams (or "metric ton")	1.103	short tons (2000 lb)	T
		TEMPERATURE (exact degrees)		
°C	Celsius	1.8C+32	Fahrenheit	°F
		ILLUMINATION		
lx	lux	0.0929	foot-candles	fc
cd/m^2	$candela/m^2$	0.2919	foot-Lamberts	fl
		FORCE and PRESSURE or STRESS		
N	newtons	0.225	poundforce	lbf
kPa	kilopascals	0.145	poundforce per square inch	lbf/in^2

*SI is the symbol for the International System of Units. Appropriate rounding should be made to comply with Section 4 of ASTM E380.
(Revised March 2003)

TABLE OF CONTENTS

LIST OF FIGURES

LIST OF TABLES

ACKNOWLEDGMENTS

The authors would like to acknowledge the valuable contributions and collaboration of Marc Eberhard and Jeffrey Berman at the University of Washington and Nasser Marafi at Risk Management Solutions for their input on the analysis methods of this project. The research presented here builds upon initial analyses performed by University of Washington and Washington State University on jointly funded WSDOT and US FHWA PACTRANS University Transportation Center projects.

Additionally, the authors would like to thank the graduate students who assisted in parts of the modeling or analysis efforts, including Zachary Kortum at the University of Washington and Stacia Bell at Washington State University. Lastly, thanks are extended to WSDOT engineers Amy Leland, Chase Weeks, Geoff Sweet, and Bijan Khaleghi for providing valuable assistance in accessing the WSDOT database and advice on current and historical WSDOT bridge design practices.

EXECUTIVE SUMMARY

The seismic performance of bridges is essential to the post-earthquake mobility of nearly all transportation modes, as bridges are relied upon to carry goods and people into and out of urban centers after natural disasters. Recent research has discovered that the Cascadia Subduction Zone (CSZ), which lies off the western coast of Washington, Oregon, and Alaska, has the potential to generate magnitude 9 (M9) earthquakes that could result in damage to the bridge network. This project used the WSDOT bridge inventory to expand an existing bridge database to include the structural properties of 58 additional bridges located on secondary state routes in Western Washington that connect to the I-5/405/90 lifeline routes. These additional bridge properties were used to define the parameters for a parametric study investigating the effects of an M9 Cascadia Subduction Zone earthquake on the bridge functionality in Western Washington. Such estimates of bridge functionality can be used to aid in the development of emergency response plans.

Research Process

The estimated functionality of bridges across Western Washington was estimated as follows:

- WSU researchers updated an existing database of bridge properties with the information of 58 additional bridges along state routes 101, 12, 16, and 3.
- The multi-span reinforced concrete column bridges were idealized with a single degree-of-freedom model following the procedure described by Kortum et al. (2021). The cyclic force-deformation response of the bridge columns was represented with a modified Ibarra-Medina-Krawinkler model that was calibrated to test results from the UW-PEER column performance database by Kortum et al. (2021).

- The range of bridges in the WSDOT bridge database was captured by using 21 single degree-of-freedom models with fundamental periods ranging from 0.1 to 4.0 seconds.
- The models were analyzed at ten locations in Washington state. At each location, 60 ground motion simulations were conducted. These were the x-y pairs of 30 simulated M9 Cascadia Subduction Zone earthquakes created by the United States Geological Survey (USGS) and the University of Washington (Frankel et al. 2018).
- The deformation demands and damage likelihood were estimated for multi-column and single-column bents. The likelihood of damage and predicted post-earthquake functionality were determined by using peak deformation demand limits from the Washington Bridge Design Manual.
- Updated bridge functionality maps were created for median and 84th percentile predicted bridge functionality along state routes 101, 12, 16, and 3.

Conclusions

The evaluation of bridge models representative of bridges along secondary routes resulted in several conclusions that can assist WSDOT and Washington state officials in emergency planning for a possible M9 CSZ earthquake.

- The characteristics of the secondary route bridges are largely similar to those of the lifeline route bridges, with the exception that secondary route bridges are generally smaller and, therefore, have smaller average column diameters of 10 to 20 inches in comparison to 30 to 40 inches. Bridge construction years, configurations, periods, and numbers of spans are all similar. Only one secondary route bridge added to the database had been seismically retrofitted with steel jackets.

- Post-earthquake bridge functionality is likely to be considerably better than that predicted by the Department of Homeland Security's *Regional Resiliency Assessment Program* (RRAP) report (2019), with most bridges along the coast likely to need repair but still useable for emergency vehicles and post-earthquake response.
- Most bridges located inland and outside of sedimentary basins were predicted to be capable of full service post-earthquake. This means that routes across the Cascade mountains should be fully open.
- For inland regions within the sedimentary basins, such as Seattle, bridges with periods of between 1.0 and 3.0 seconds would likely sustain moderate damage, resulting in limited service. Short period bridges in these regions would likely be able to retain full service.
- Port Angeles, Forks, and Ocean Shores are the regions of Western Washington with the highest probability of significant bridge damage. At these locations, the probability of exceeding a displacement ductility demand of 2.0, which is the limit for minor damage requiring little-to-no repair, was found to be greater than 40 percent for most periods of less than 3.0 seconds.
- The likelihood of significant damage, collapse, or total loss of service post-earthquake was found to be below 20 percent for all regions of Western Washington, except Port Angeles.

Limitations

The results of this research project come with several limitations that could be alleviated by further research or more detailed, bridge specific analysis.

- The analyses did not account for the resistance of the abutments.

- The analyses did not consider the effect of soil stiffness. Specifically, the project assumed relatively stiff site class C soil. Site class D and E soils may further amplify the bridge response, and liquifiable soils (site class F) may cause greater damage than predicted.
- The analyses neglected failure modes of span unseating, shear failure, and foundation failures. These failure modes are brittle and could lead to collapse in older bridges. WSDOT retrofit efforts and design practices have taken steps to limit span unseating and shear failure modes.

CHAPTER 1. INTRODUCTION

Many bridges in the western United States, including those built during the Interstate Highway Program in the 1950s and 1960s, are seismically vulnerable to strong ground motions. The seismic performance of many of these bridges is essential to the post-earthquake mobility of nearly all transportation modes, as bridges are relied upon to carry goods and people into and out of urban centers after natural disasters. Damage to bridges near critical facilities, such as airports and ports, can also delay the post-earthquake emergency response and mobility of people, freight, and supplies. Accordingly, local, state, and federal agencies are interested in estimating post-earthquake bridge functionality to plan for disaster mitigation, post-event response, and long-term recovery. Current estimates for the post-earthquake bridge functionality in Washington following a Magnitude 9.0 (M9) Cascadia Subduction Zone (CSZ) earthquake (e.g., DHS, 2019) are inadequate because of overly simplistic predictions of bridge response. The current estimate is that 80 percent of the bridges in Western Washington would be non-functional following an M9 earthquake, which is likely inaccurate and over-predicts the amount of damage that would be caused by a CSZ earthquake. Because the Department of Homeland Security (DHS) Regional Resiliency Assessment Program (RRAP) study (2019) predicts such widespread and high levels of bridge damage, the recommended response and recovery plan is heavily reliant on air transportation to provide resources to the affected populations. However, surface transportation modes, if available, are better suited for moving large volumes of resources and serving as critical lifeline routes for impacted regions of the state (DHS, 2019).

The lack of accuracy provided by current post-earthquake evaluations stems, in large part, from the lack of available data about the characteristics of the Washington bridge inventory. Models that were developed from more accurate data about the characteristics of the bridge inventory would enable more reliable estimates of post-earthquake bridge functionality and

would provide authorities with better data from which to make policy and planning decisions. The goal of this study was to create an improved map of predicted bridge functionality for routes in Western Washington that connect to the WSDOT lifeline routes of I-5, I-405, and I-90. This goal would assist in post-earthquake emergency planning because it is hypothesized that the majority of the bridges would be capable of at least emergency levels of functionality, allowing officials to use surface transportation modes for disaster response. This research focused on the modeling and functionality of bridges along the secondary routes that connect to the main WSDOT lifeline corridors because other research, conducted by the University of Washington, Washington State University, and WSDOT, has already focused on the lifeline routes of I-5/405/90. Knowing the predicted post-earthquake conditions of the secondary routes is important for gauging the likelihood of mobility for emergency management plans.

This report begins with a brief overview of the background information surrounding the CSZ earthquake. Then, the methodology used to model the bridge network in Western Washington, based on data obtained from WSDOT's bridge inventory database, is described. Lastly, the model analysis results are described, and several scenarios of predicted bridge network functionality are presented.

CHAPTER 2. BACKGROUND

2.1. Magnitude 9 Cascadia Subduction Zone Simulations

Recent research into the Cascadia Subduction Zone (CSZ), which is a 600-mile-long tectonic plate boundary between the North American plate and Juan de Fuca plate, shown in figure 2.1, has indicated that it is capable of producing a large magnitude earthquake at a return period of approximately 400-600 years (Pacific Northwest Seismic Network, 2021). Studies on previous subduction zone earthquakes, predominately near Chile and Japan, have shown that these earthquakes can have larger spectral accelerations and durations than typical crustal earthquakes. These effects may be further amplified by sedimentary basins located around Western Washington (Marafi et al., 2017). Researchers from the United States Geological Survey (USGS) and the University of Washington (UW) simulated a magnitude-9 rupture of the CSZ using synthetic seismograms and 3D finite difference simulations (Frankel et al., 2018). The joint research program resulted in 30 sets of synthetic ground motions across a range of possible rupture parameters. The generated M9 motions had durations ranging from 70 to 120 seconds, with the largest spectral accelerations occurring near the Pacific Coast (Frankel et al., 2018). Spectral accelerations were amplified by the presence of sedimentary basins around the Seattle and Olympia areas.

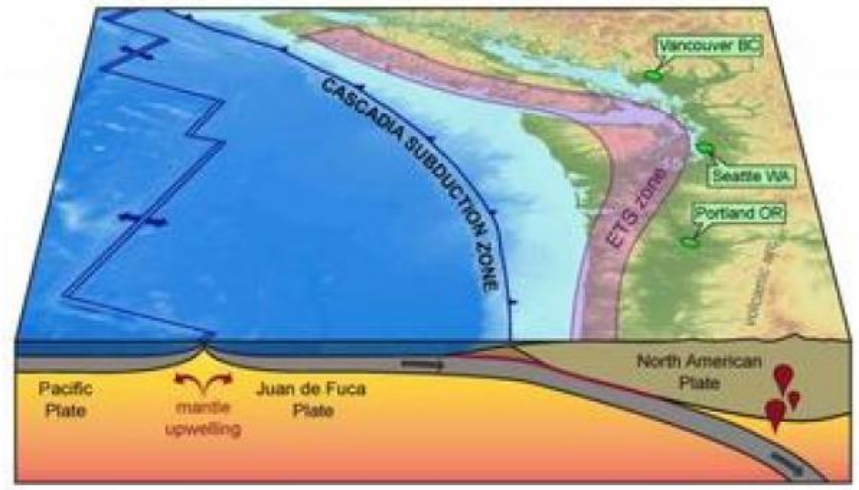

Figure 2.1. The Cascadia Subduction Zone (Public domain image).

Marafi et al. (2020) investigated the effects of the CSZ motions on tall, reinforced concrete core wall buildings, finding that buildings located within the Seattle basin were subjected to large spectral acceleration, damaging spectral shapes, and longer durations of shaking. The collapse probability of these buildings, designed to minimum standard code, averaged 27 percent (Marafi et al., 2020). Similarly, Chandramohan et al. (2019) investigated the effect of ground motion duration on the collapse of reinforced concrete bridge piers and found that long-duration motions were correlated to a 17 percent decrease in collapse capacity in comparison to typical short-duration motions. Lastly, De Zamacona (2019) investigated the effects of the simulated, soil-adjusted M9 CSZ motions on different single degree-of-freedom models. Some models were assumed to have a strength 50 percent higher than the 2019 WSDOT minimum code value for bridges, and those models predicted severe damage for short-period structures that were close to the fault. Longer-period structures were more heavily damaged if located within the sedimentary basins.

2.2. 2019 Department of Homeland Security RRAP Report

The Department of Homeland Security Regional Resiliency Assessment Program (RRAP) study (DHS, 2019) attempted to assess the functionality of approximately 2,700 bridges in Western Washington following an M9 CSZ earthquake. The findings of this study grimly predicted that large percentages of bridges across Washington would be completely destroyed or otherwise unusable post-earthquake. This conclusion is partially summarized in figure 2.2, in which the predicted reopening times for each bridge across Western Washington are provided. As shown by the figure, most of the bridges were predicted to be out of service for greater than one year, which has been factored into the emergency planning efforts in Washington state. Specifically, this study projected that approximately 80 percent of the bridges in Western Washington would be unavailable following an M9 CSZ earthquake, and 782 bridges would be unavailable for more than one year. However, these estimates are unreliable because of the lack of underlying data used, such as the following:

- The study relied on metrics of ground-motion intensity that correlated poorly with bridge performance (e.g., peak ground acceleration rather than effective spectral acceleration).
- The study relied heavily on crude fragility relationships that were not consistent with the level of damage observed in past earthquakes (Ranf, et al., 2007), fragility relationships developed by previous researchers (e.g., Gidaris et al., 2017), or damage and functionality expected by WSDOT based on the Washington Bridge Design Manual (BDM) (WSDOT, 2020).
- The study did not consider specific bridge characteristics, specifically fundamental period, when predicting performance.

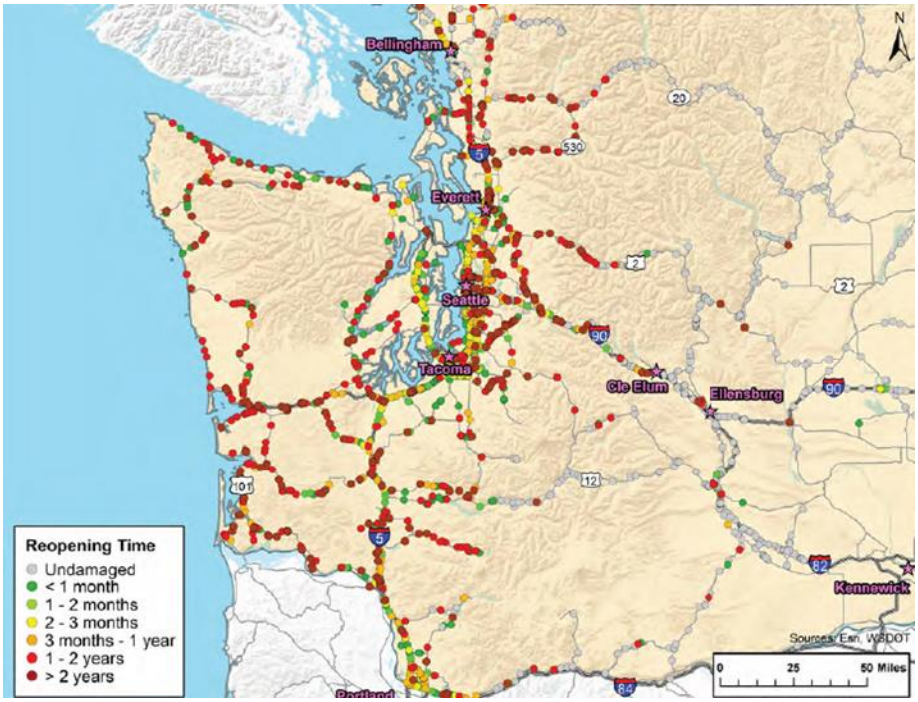

Figure 2.2. Reopening times in Western Washington proejcted by the DHS RRAP report (DHS, 2019)

This study was intended to rectify many of these analytical shortcomings to provide more accurate predictions of bridge functionality.

2.3. Impacts of a CSZ Earthquake on Washington State Bridges

A recent study conducted by researchers at the University of Washington (UW) evaluated the predicted deformation demand of bridge columns for various locations around Western Washington (Kortum et al., 2021). The study used a database of 609 bridge properties located mostly along the I-5/405 lifeline corridors that was compiled from WSDOT's bridge inventory. From the bridge property database, researchers developed 18 nonlinear single degree-of-freedom models that reasonably well represented the spread of bridge period, stiffness, and strength. These models were analyzed at ten locations across Western Washington for the 30 M9 CSZ

scenarios for four different site classes. From the analyses, several significant conclusions were reached (Kortum et al., 2021):

- Approximately 75 percent of the lifeline bridges were designed before 1976, which is when earthquake design standards for bridge columns changed significantly in response to the 1971 San Fernando, California, earthquake. Post-1976 bridges are expected to be more ductile than pre-1976 bridges.
- On soft soils, bridges with periods of above 0.4 to 0.7 seconds had the largest spectral accelerations, deformation demand, and expected damage. For stiffer soils, bridges with shorter periods tended to have the highest demands.
- Bridges with strength of one standard deviation below the median had deformation demands approximately 50 percent larger than bridges of median strength.
- While there are no deep sedimentary basins along the Pacific Coast of Washington state, the acceleration response spectra for the coast were very high, with values near 2.0g. For bridges with periods of between 0.2 and 2.0 seconds, the predicted likelihood of concrete spalling was from 35 to 50 percent for site class C soil.
- For bridges located away from the CSZ and outside of sedimentary basins, the spectral acceleration was low, ranging from 0.5g to 1.0g, and the likelihood of concrete damage was low for all conditions.
- For bridges within sedimentary basins, performance was strongly linked to the fundamental period. For bridges with periods of between 0.5 and 3 seconds, the likelihood of concrete spalling was between 50 and 75 percent.

The study presented here was largely completed in collaboration with the UW research team. The modeling procedure and ground motions used in this research aligned with the UW

research to ensure that the results were comparable and relevant. This research extended the previous UW study to link specific bridges in the expanded WSDOT database to predicted functionality based on the WSDOT BDM (WSDOT 2020) ductility demand limits. The goal was to create functionality maps that could be compared to the maps shown in the DHS RRAP report.

CHAPTER 3. DATA AND METHODS

This project used single degree-of-freedom (SDOF) models that represented typical pre-1976 bridges in Washington state to evaluate the likelihood of damage to bridges along secondary routes following an M9 Cascadia Subduction Zone earthquake. The CSZ was simulated by using 30 M9 scenarios for ten locations around Western Washington. The likelihood of bridge damage was predicted by using the estimated bridge period, based on its approximate mass and lateral stiffness, bridge location, and bridge fragility from the Washington BDM. The study considered only ductile failure and did not consider failure modes of span unseating, shear failure, longitudinal bar fatigue, foundation failure, or site liquefaction. Additionally, the models did not consider the resistance provided by the abutments. The secondary routes considered were mostly to the west of I-5 along state routes 101, 12, 16, and 3, which are all in areas of Washington state that are likely to see significant shaking during a CSZ earthquake. The remainder of this chapter describes the approach used to predict bridge performance and functionality.

3.1. Expansion of the WSDOT Bridge Database

The Washington State Department of Transportation (WSDOT) has compiled a database of bridge properties along the primary lifeline routes of I-5, I-405, and I-90 between Seattle and Snoqualmie. The majority of the information known about bridge properties across Washington were derived from this database, which comprised information from 609 highway bridges, located as shown in figure 3.1. For each bridge in the WSDOT database, the parameters collected were year of construction, superstructure type, column dimension, transverse and longitudinal reinforcement ratio, span length, and number of piers. Column properties were only provided for the tallest and shortest columns on the bridge.

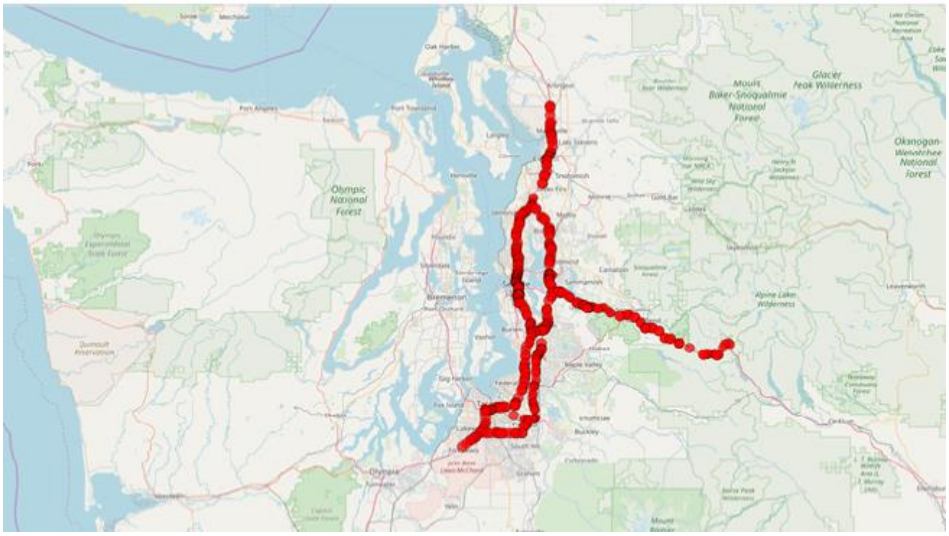

Figure 3.1. Locations of lifeline route bridges along I-5, I-405, and I-90 (from Kortum et al. 2021).

This project expanded the existing WSDOT bridge database to include the parameters of 58 additional multi-span, reinforced concrete column bridges on secondary routes, including state routes (SR) 101, 12, 16, and 3, as shown in Figure 3.2. The characteristics of these secondary route bridges were analyzed and compared to the typical characteristics of bridges from the lifeline routes, which were summarized by Kortum et al. (2021). The expansion of the WSDOT bridge database excluded single-span bridges, which would likely survive any earthquake if unseating and abutment failure were prevented, pier wall bridges, steel truss bridges, and special project bridges, such as suspension bridges.

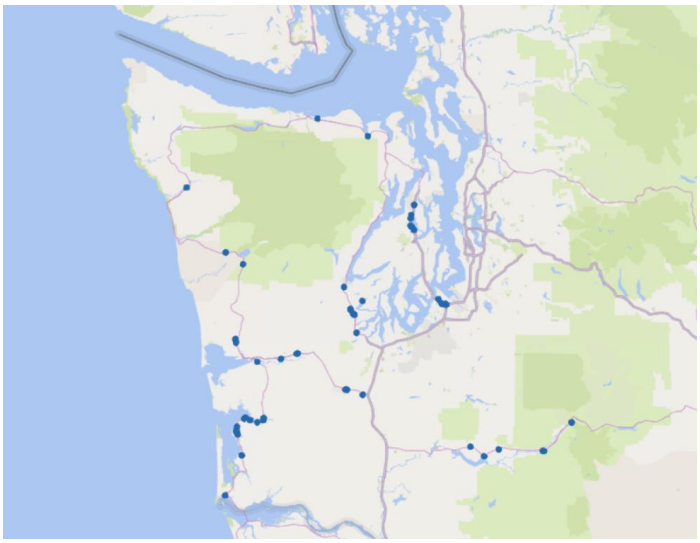

Figure 3.2. Locations of additional multi-span bridges

The characteristics of the bridges were important for generating estimates of structural properties, such as stiffness, strength, period of vibration, and ductility. The additional 58 bridges added to the database ranged in year of construction from 1948 to 2018, with 48 percent built before 1976. Approximately 75 percent of the I-5/405/90 lifeline bridges were constructed before 1976. The year 1976 is important in seismic engineering, as it is the year in which seismic detailing of reinforced concrete columns was significantly improved in response to the 1971 San Fernando, California, earthquake. Therefore, bridges designed after 1976 are likely to be more capable of resisting larger deformations than pre-1976 bridges.

Of the multi-span bridges on the secondary routes examined, five of the 58 were supported by single-column bents, while the rest were supported by multi-column bents. Single-column bridge bents have less redundancy because of a lower ability to redistribute force through the formation of plastic hinges. Because of this, the Washington BDM (WSDOT 2020) predicts lower peak ductility capacity for single-column bents than for multi-column bents.

Column height and diameter affect column stiffness. The majority of the secondary route bridges were similar to the lifeline route bridges, with average column heights of between 6 to 30 feet. Three had column heights of greater than 40 feet. The secondary route bridges had common column diameters of between 11 and 20 inches, which were smaller diameters than those of the lifeline route bridges, which were more commonly between 31 and 40 inches. Only one secondary route bridge added to the database had been seismically retrofitted with steel jackets.

Although longitudinal reinforcement ratio, which is the ratio of the area of longitudinal steel reinforcement to the gross area of the column cross-section, varied widely, all but three of the secondary route bridges had longitudinal reinforcement ratio between 0.5 and 3.5 percent. None of the pre-1976 bridges had a longitudinal reinforcement ratio of greater than 3.0 percent. Similarly, 80 percent of the bridges had a transverse reinforcement ratio of less than 0.5 percent. The most common bridge configuration was three spans. All of these parameters matched well with those of the lifeline route bridges. In conclusion, the secondary route bridges were largely similar to the lifeline route bridges, with the exception of smaller column diameters and a prevalence of multi-column bents over single-column bents.

Using the information in the bridge database and the methodology described by Kortum et al. (2021), each bridge's weight, lateral stiffness, and fundamental period of vibration were estimated. First, the bridge mass was estimated by using a relationship between bridge longest span length and weight per square foot of bridge deck. This relationship was developed for each common superstructure type—which for the secondary route bridges were prestressed girder bridges and slab bridges—by going through the structural drawings of a selected subset of the bridges to calculate total bridge mass divided by the bridge deck area. Total bridge weight was calculated excluding the column weight and assumed a concrete unit weight with reinforcement

of 150 lb/ft^3. Figure 3.3 shows this relationship for each type of bridge superstructure and the fit of the relationships to the data, with blue dots being bridge weights calculated by the UW from the main lifeline corridor database and red dots being bridge weights calculated by this research team for secondary route bridges. As shown in figure 3.3, there was reasonably good correlation between longest span and bridge weight, which were used to estimate the bridge weights for the remainder of the bridges in the expanded database.

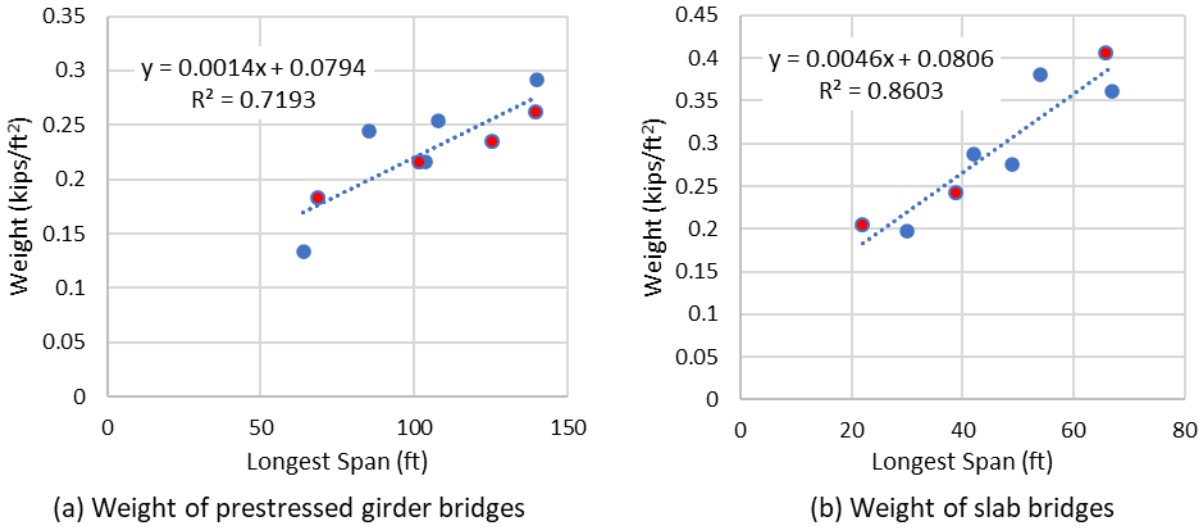

Figure 3.3. Approximate relationship between bridge weight per square foot and longest span

The next property calculated was the total lateral stiffness provided by the columns. However, the WSDOT database provided only the column properties needed to calculate stiffness for the shortest and longest columns. Therefore, the total stiffness was estimated by using these properties and a correction weighting factor alpha (α). The column weighting factor was defined by Kortum et al. (2021) as, "the proportion of columns on the bridge that were treated as having properties of the shortest bridge column, where $0 < \alpha < 1$." Alpha was calculated to be 0.5 for bridges with two piers, 0.4 for bridges with three piers, and 0.33 for

bridges with four or more piers. The stiffness of a single column was calculated by using the effective column stiffness at yield from Elwood and Eberhard (2009), that is:

$$\frac{EI_{eff,calc}}{EI_g} = \frac{0.45+2.5P/A_g f_c'}{1+110\left(d_b/D\right)\left(D/a\right)} \leq 1.0 \text{ and } \geq 0.2 \quad (1)$$

where P is the column axial load, A_g is the gross column area, f'_c is the nominal concrete compressive stress, d_b is the nominal longitudinal reinforcement bar diameter, D is the column diameter, and a is the shear span. This effective column stiffness accounts for column flexural, shear, and bond slip flexibility. Column stiffness was calculated for both a fixed-fixed boundary condition and a fixed-pin boundary condition, as both would be possible, depending on the fixity of the top of the column and the foundation system and soil stiffness. Columns with deep foundations in shallow rock would behave more fixed, while columns with shallow footings on softer soils would behave more like a pin. The total lateral stiffness was then calculated with the alpha factor and the total number of bridge columns, as:

$$K_{bridge} = \#_{cols}[\alpha K_{short} + (1-\alpha)K_{tall}] \quad (2)$$

where K is the stiffness, and $\#_{cols}$ is the total number of columns supporting the bridge. Lastly, period was calculated by using the above estimates for stiffness, K_{bridge}, and mass, M_{bridge}, for both a fixed-fixed and fixed-pin boundary condition for all 58 bridges in the expanded database, as:

$$T_{bridge} = 2\pi\sqrt{K_{bridge}/M_{bridge}} \quad (3)$$

Figure 3.4 shows the range of bridge periods depending on boundary condition assumption for the 58 bridges on the secondary routes. It is apparent that the majority of bridges had periods of less than 1.5 seconds for either boundary condition. The fixed-pin boundary condition resulted in higher periods because of greater column flexibility. These bridge periods aligned closely with the bridge periods calculated for the lifeline route bridges, for which 70 percent fell between a period of 0.25 and 0.75 seconds for a fixed-fixed boundary condition and 50 percent fell between a period of 0.75 and 1.25 seconds for a fixed-pin boundary condition (Kortum et al., 2021).

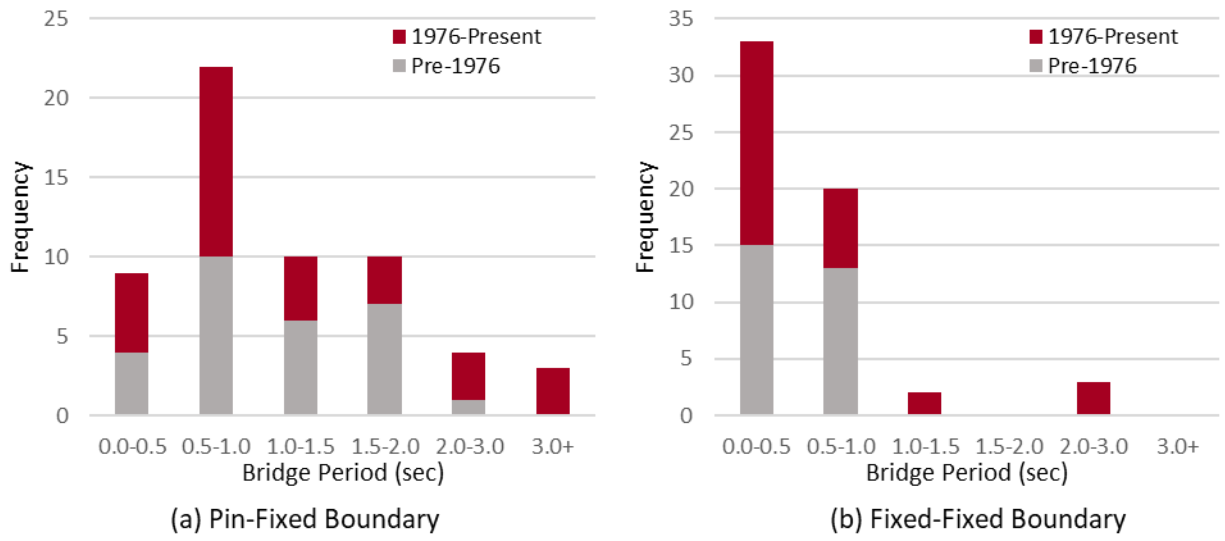

Figure 3.4. Estimated bridge periods for 58 bridges on secondary routes

The last property needed to create the SDOF models was normalized base shear. Since strength and stiffness of structures are roughly proportional, there is a relationship between bridge period and strength. This relationship was developed by Kortum et al. (2021) into two curves that relate bridge period to the normalized bridge base shear strength per unit weight, F_y/W, for pre-1976 and post-1976 bridges. The differences between the two curves were found to

be minimal and only affected the normalized base shear strength of bridges with periods of less than 0.5 seconds. For short period bridges, Kortum et al. determined that the design strength of post-1976 bridges was higher than that of pre-1976 bridges, which would make them less susceptible to larger deformations and damage. This project assumed a conservative strength, and only the relationship developed for pre-1976 bridges was used, as shown by figure 3.5. Figure 3.5 shows the fit of all the bridges in the lifeline route database to the relationship for both the fixed-fixed and fixed-pin boundary conditions. This relationship is numerically described by Equation (4) and was used to determine the average base shear strength of the SDOF models for a given period.

$$\frac{F_y}{W} = max\left(0.07, min\left({}^{0.20}/_{T}, 0.86\right)\right) \quad (4)$$

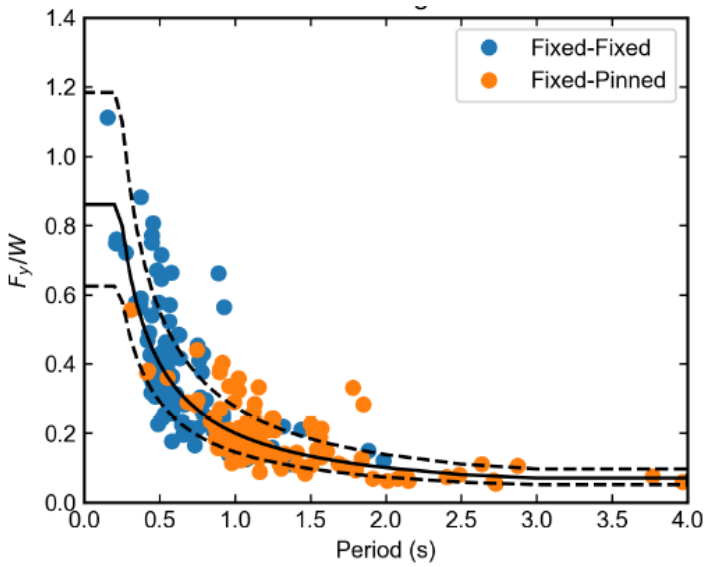

Figure 3.5. Normalized base shear strength versus period for pre-1976 bridges, with curve fit based on mean and mean +/- one standard deviation (Kortum et al., 2021)

3.2. Nonlinear SDOF Bridge Model

The response of the bridges was represented with a nonlinear single degree of freedom model that used the Modified Ibarra-Medina-Krawinkler (IMK) deterioration model with peak-oriented hysteretic response material (Lignos and Krawinkler, 2012; Kortum et al., 2021). The IMK model, shown by figure 3.6, uses several input parameters to control the backbone of the force-displacement behavior. These parameters were calibrated by Kortum et al. (2021) to match the measured force-displacement response of reinforced concrete column tests in the UW-PEER structural performance database. The same IMK modeling procedure described by Kortum et al. (2021) was used to characterize the bridges from the secondary routes for this study. In total, 21 variations of the bridge model were used to represent a range of bridges with periods of 0.1 seconds to 4.0 seconds.

The IMK model captured four modes of deterioration, which were unloading stiffness deterioration, strength deterioration, post-capping strength deterioration, and reloading stiffness deterioration. The rate of deterioration was controlled for each mode by λ and an exponent *c*. Haselton et al. (2008) and Kortum et al. (2021) recommended assuming that the λ for each mode was the same and setting *c* equal to 1.0 for all modes. In using this assumption for λ, eight parameters were necessary to calibrate the IMK model, which were as follows:

1. Yield strength, M_y, for each column was calculated for each period by using Equation (4) and a unit mass.
2. Elastic stiffness was calculated by using the relationship between period, stiffness, and mass shown by Equation (3). For the SDOF models, the elastic stiffness was calculated as: $K = \left({}^{2\pi}/_{T}\right)^2 M$.
3. Post-yield stiffness was assumed to be a constant 5 percent of the elastic stiffness.

4. The post-capping negative tangent stiffness was assumed to be 10 percent of the elastic stiffness, and this was used to calculate θ_{pc}.
5. The ultimate rotation, θ_u, was taken as 100 times the sum of θ_y, θ_p, and θ_{pc} to prevent modeling convergence issues.
6. The residual strength M_r, was set equal to 1 percent of the yield strength.
7. λ was taken as 100 per recommendations from Kortum et al. (2021) for the low values of transverse reinforcement ratio in the columns in the expanded database.
8. To calculate θ_p, the ratio of θ_p/θ_y was taken as 5.0 for all models based on recommendations from Kortum et al. (2021). This assumed that columns would respond in a fairly ductile manner, reaching 5.0 times their yield rotation before significant degradation.

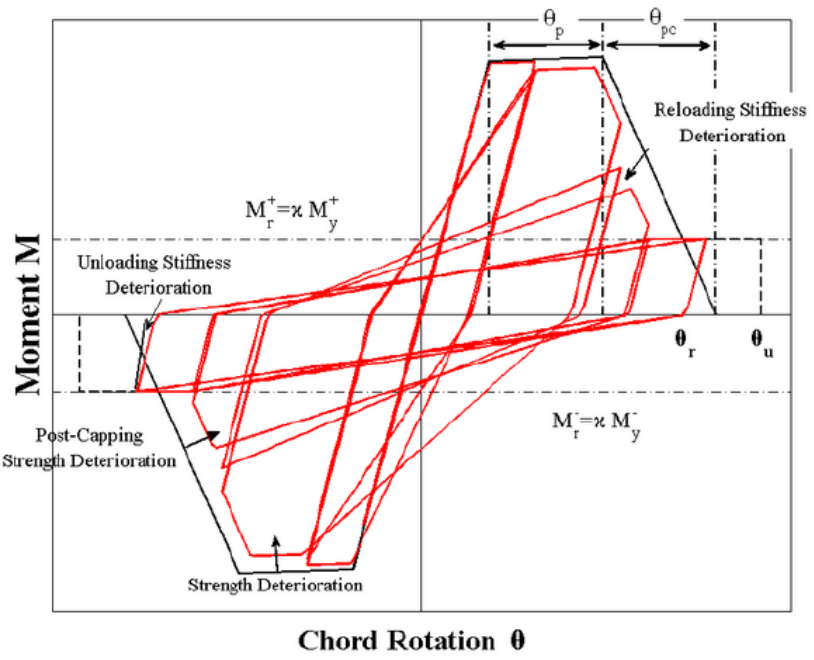

Figure 3.6. IMK model backbone (Lignos and Krawinkler, 2012)

Using this modeling procedure, Kortum et al. (2021) compared the IMK model results with three experimental tests from the UW-PEER database. The three tests comprised a lightly reinforced column, a moderately reinforced column, and a heavily reinforced column, as shown in Figure 3.7. In general, the IMK models accurately predicted the cyclic behavior and deterioration of the column tests, and so they were deemed sufficiently accurate for this study.

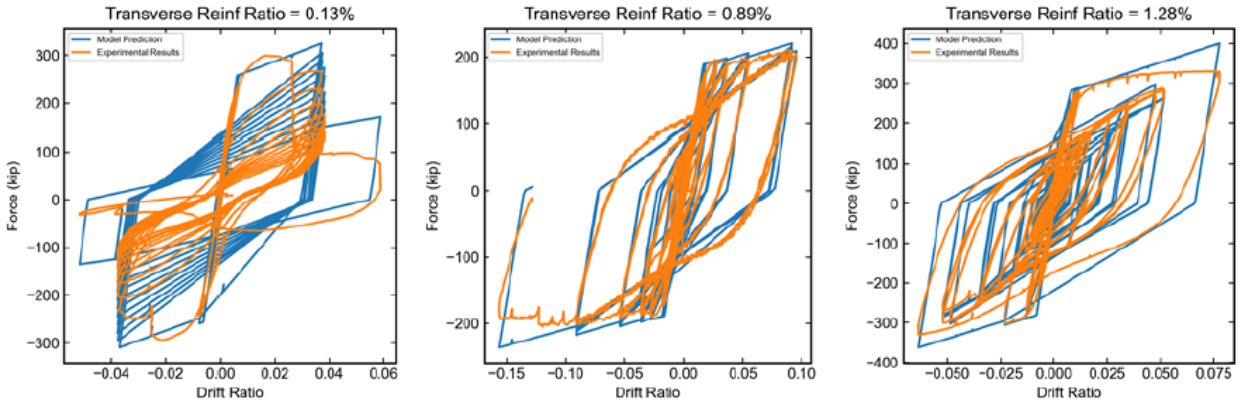

Figure 3.7. Fit of IMK model to column tests with different transverse reinforcement ratios (Kortum et al. 2021).

3.3. CSZ Ground Motions Used for Analysis

Once the 21 SDOF bridge models had been established, they were analyzed for the set of 30 simulated CSZ ground motions at ten locations across Western Washington, with each motion at each location containing two orthogonal components. The simulated motions used were the baseline motions from Kortum et al. (2021), which had a soil shear-wave velocity in the top 30 meters, V_{s30}, of 600 m/s, which approximately corresponded to National Earthquake Hazards Reduction Program (NEHRP) site class C. The locations of the ten sites are shown in figure 3.8 and described in table 3.1. Figure 3.9 shows the median response spectra for each of the ten sites, divided by site characteristics of whether they were coastal or inland and if they were in or outside of a sedimentary basin. As shown by figure 3.9, the coastal cities of Forks and Ocean

Shores, where many of the secondary routes analyzed in this study were located, had high spectral accelerations at periods of 0 to 1 second. Additionally, the effect of the sedimentary basins was evident between periods of 1 to 3 seconds, at which the spectral acceleration maintained a relatively high value before decreasing.

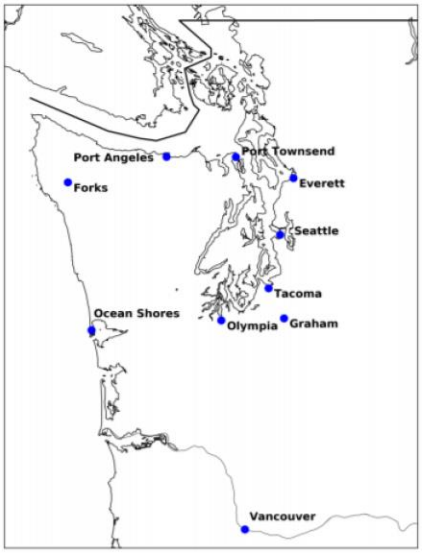

Figure 3.8. Locations of the ten sites for analysis (De Zamacona, 2019).

Table 3.1. Selected sites and nearest station (from Frankel et al. 2018).

City Name	Station ID	Latitude	Longitude
Forks	Z0FORK	47.9456	-124.566
Ocean Shores	Z0XOCS	46.9778	-124.154
Port Angeles	Z0XANG	48.1191	-123.431
Olympia	Z00CPW	46.9717	-123.138
Port Townsend	Z0XTWN	48.1146	-122.756
Vancouver	Z0HUBA	45.6287	-122.653
Tacoma	Z0TBPA	47.2559	-122.368
Seattle	Z0XWLK	47.6120	-122.338
Graham	Z00GHW	47.0395	-122.274
Everett	Z0EVCC	48.0056	-122.204

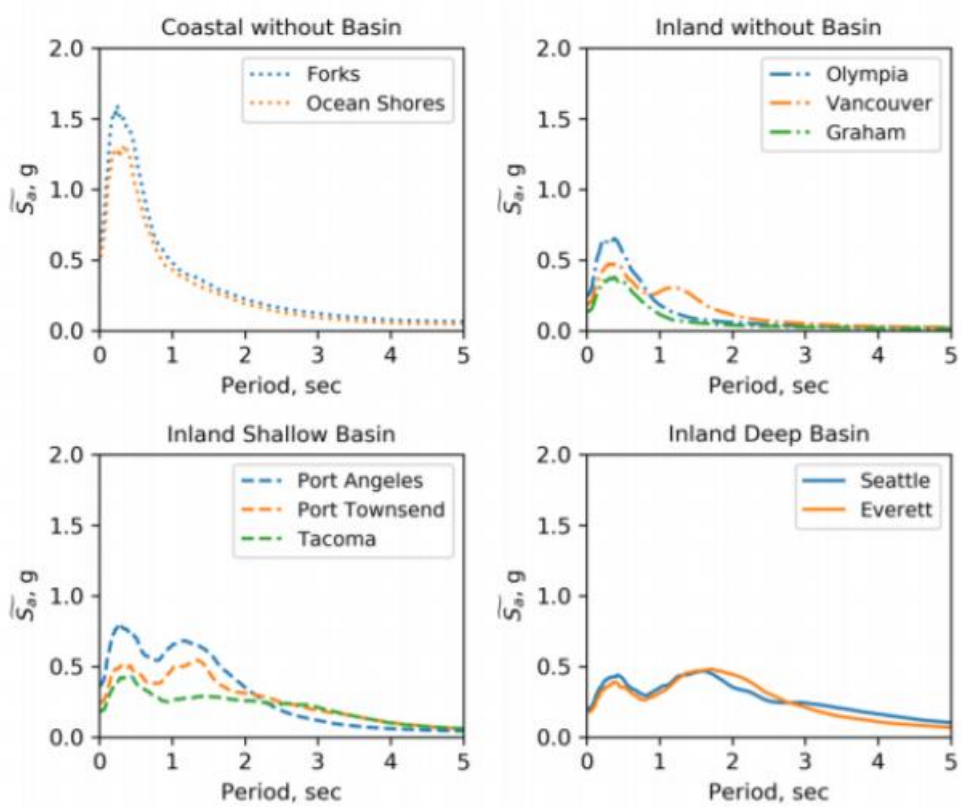

Figure 3.9. Response spectra of ten sites (De Zamacona, 2019).

3.4. Predicting Bridge Functionality

Bridge functionality was predicted by using the ductility ratio of maximum displacement / yield displacement (D/D_y) and the expected bridge seismic performance criteria defined by the Washington BDM (WSDOT 2020). The BDM has four expected post-earthquake damage states:

1) None – no damage,
2) Minimal – essentially elastic performance with flexural cracking and minor spalling,
3) Moderate – bridge repair is likely, but bridge replacement is unlikely, extensive cracking and spalling with visible reinforcing bars, and
4) Significant – onset of failure of core concrete, bridge replacement is likely as all plastic hinges have formed with ductility demand approaching limits.

These damage state levels are most applicable to post-1976 and modern column designs. However, they were used by Kortum et al. (2021) for all analyses and were likewise applied to all bridges in the extended database in this study. This assumed that the pre-1976 bridges would fail in a flexural hinging manner, not through shear failure or foundation failure. WSDOT has an ongoing seismic retrofit program to retrofit shear critical columns with steel or fiber-reinforced polymer jackets to prevent shear failure.

In the BDM, the expected post-earthquake damage states are then related to three expected post-earthquake service levels, depending on the seismic critical member. For this project, the seismic critical member for all the bridges was either single-column bent or multiple-column bent. The three expected post-earthquake service levels we as follows:

1) Full service – full access to ordinary traffic is available almost immediately after the earthquake,
2) Limited service – the bridge is open for emergency vehicle traffic, and reduced number of lanes for ordinary traffic is available within three months of the earthquake, and
3) No service – the bridge is closed for repairs and replacement.

Since expected post-earthquake bridge service is the more critical finding for emergency planning, it was used as the primary reporting measure for this study. Full service bridges would be open for emergency vehicles, evacuations, and movement of supplies directly after the earthquake. Limited service bridges would likely be open for emergency vehicles and movement of supplies for emergency response but would not be open for traditional traffic until approximately 3 months post-earthquake. No service bridges are assumed to be non-functional and, therefore, would prevent the passage of any vehicle. On the basis of Table 4.1-2 in the

Washington BDM, the bridge functionality limits for expected post-earthquake service are summarized in table 3.2.

Table 3.1. Bridge functionality and service level ductility demand limits.

Critical member type	**Full Service**	**Limited Service**	**No Service**
Single column bents	$0 < D/D_y < 1.5$	$1.5 \leq D/D_y < 5.0$	$5.0 \leq D/D_y$
Multiple column bents	$0 < D/D_y < 2.0$	$2.0 \leq D/D_y < 6.0$	$6.0 \leq D/D_y$

CHAPTER 4. FINDINGS

This chapter summarizes the results of the parametric study that used SDOF models to represent the majority of multi-span bridges across Western Washington. Figure 4.1 shows the median displacement ductility demands for the ten sites analyzed across Western Washington. The figure shows that none of the locations had a ductility demand approaching the no service ductility demand level. Furthermore, some locations, such as Graham and Olympia, which are both inland and outside of the basin, did not have ductility demands exceeding the full service ductility limit for any bridge period.

Figure 4.2 shows the displacement ductility demands for the 84th percentile of the analyses, meaning 84 percent of the analyses had displacement ductility demand of less than or equal to the value shown in the figure. The 84th percentile is approximately equivalent to the mean plus one standard deviation in statistics. For the 84th percentile ductility demand, some sites, such as Port Angeles, had significant increases in peak demand, whreas other sites, such as Graham, remained relatively unchanged. This shows that variability in ductility demand from ground motion characteristics would be greater in the coastal locations, which are closer to the fault, and locations within the sedimentary basin, which would amplify the shaking. For the majority of periods and locations, the predicted service level would be limited service. However, given the 84th percentile results, bridges with periods of between 0.75 and 1.75 seconds near Port Angeles would be at risk of significant damage and no service post-earthquake. Single-column bent bridges with periods of between 1.5 and 3 seconds in Seattle would be at a similar risk of significant damage and no service.

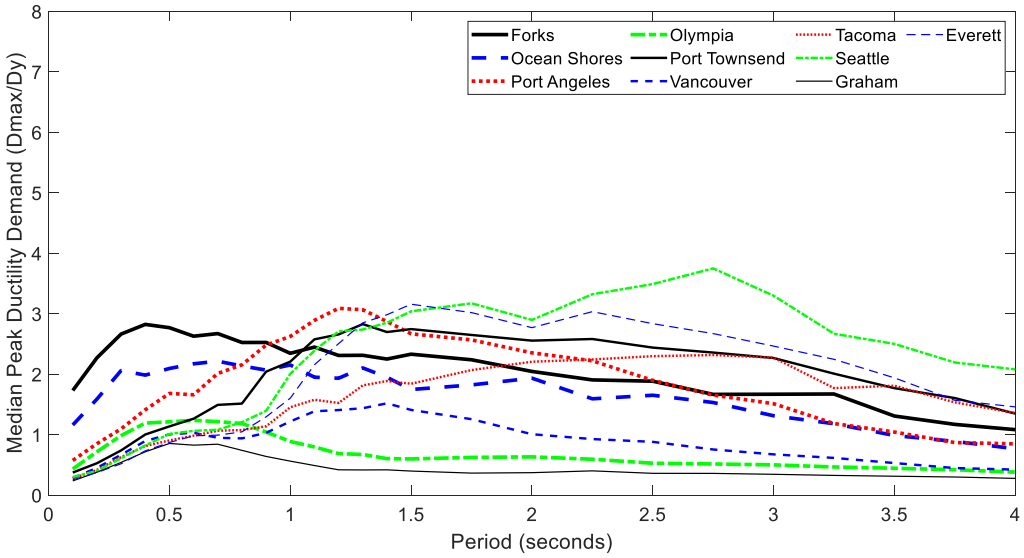

Figure 4.1. Median ductility demand of bridges across Western Washington.

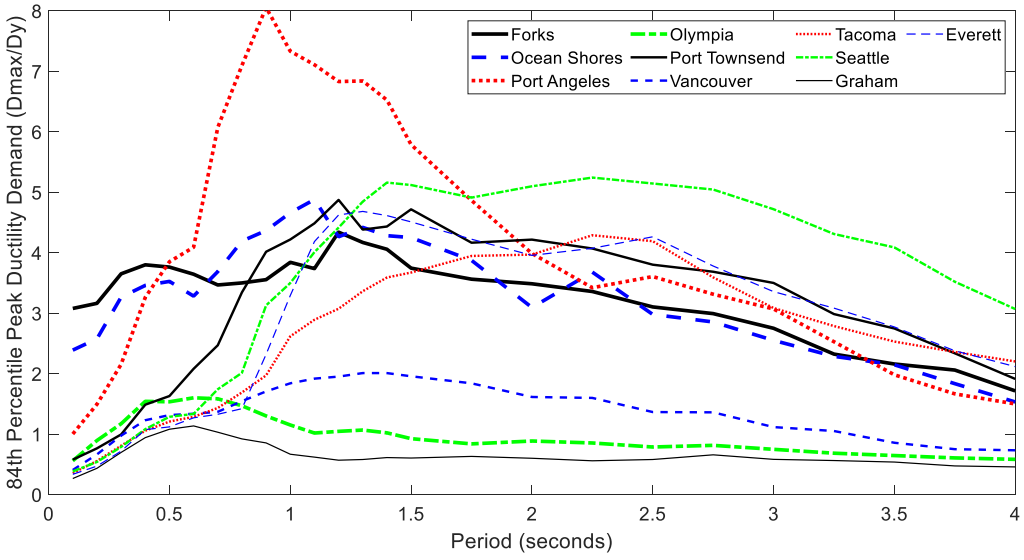

Figure 4.2. 84th percentile ductility demand at ten sites in Western Washington.

Another way to visualize the analysis results is to calculate the probability of exceeding a specific ductility demand for each location, as shown by figure 4.3 and figure 4.4. Figure 4.3 shows the probability of a bridge exceeding a ductility demand of 2.0, which is the full service limit for multiple-column bent bridges. Figure 4.4 shows the probability of a bridge exceeding a ductility demand of 5.0, which is the no service limit for single-column bent bridges. Figure 4.3 shows that short period bridges near the coastal locations of Ocean Shores and Forks would have a higher probability of sustaining enough damage to be at limited service post-earthquake than bridges at inland, non-basin locations, such as Vancouver and Graham. For inland sites with a sedimentary basin, such as Port Angeles, Port Townsend, and Seattle, the probability of exceeding ductility demand of 2.0 was found to be less than 20 percent for periods of 0.5 seconds or less. Therefore, short span bridges, bridges with short columns, and single-span bridges would likely be relatively undamaged and capable of full service, whereas the longer period bridges would be more likely to sustain damage resulting in limited service.

Figure 4.4 shows that, for almost all sites and all bridge periods, the probability of a bridge exceeding a ductility demand of 5.0, resulting in significant damage, would be less than 20 percent. For Port Angeles, bridges with periods of between 0.5 and 1.75 seconds would be most vulnerable to CSZ earthquakes, with the largest probability of significant damage, resulting in no service post-earthquake. The probability of a ductility demand of greater than 5.0, resulting in significant damage, for Seattle would be highest for bridges with periods of between 1.75 and 3.25 seconds because of the sedimentary basin effects.

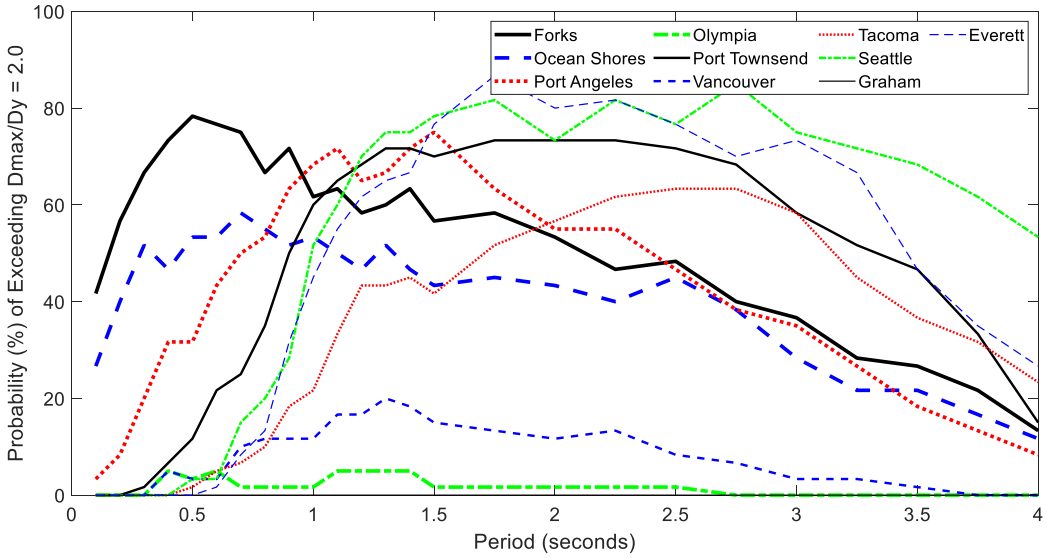

Figure 4.3. Probability of exceeding a ductility demand of 2.0

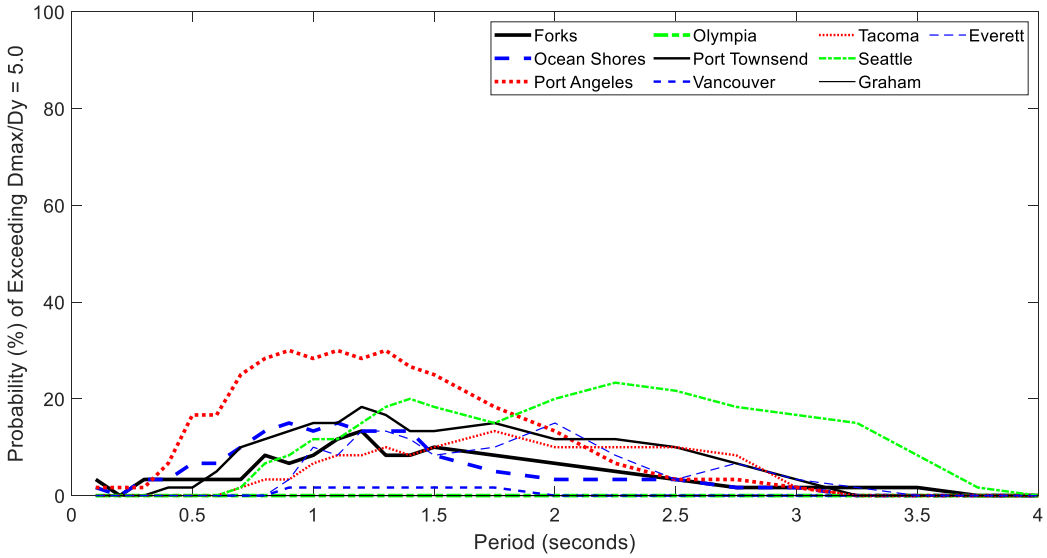

Figure 4.4. Probability of exceeding a ductility demand of 5.0

Figure 4.1 and figure 4.2 were used in conjunction with the expanded bridge database to predict the functionality of the 58 bridges on secondary routes in Western Washington. Each bridge in the database was assigned to the closest of the ten sites used for analysis. Each bridge was able to be assigned to an analysis location that was within 40 miles of the site; the average distance from bridge location to analysis location was 17.6 miles. The predicted functionality maps for each bridge are shown in figure 4.5 and Figure 4.6 for the median response curve and 84^{th} percentile response curve, respectively. For all bridges, the maps were created by using the periods estimated for both the fixed-fixed and fixed-pin boundary conditions.

Among all the cases, only one bridge located near Port Angeles was predicted to have significant damage that would result in no service post-earthquake. The trend across all the functionality maps was that limited service could be expected for bridges directly along the coast from Ocean Shores to Port Angeles. The bridges along SR 12 between the coast and Olympia in the database were all predicted to be in full service post-earthquake, meaning it is highly likely that residents and supplies could navigate from coastal communities to the WSDOT lifeline using this route. Similarly, SR 12 across the Cascade mountains was predicted to maintain full service post-earthquake.

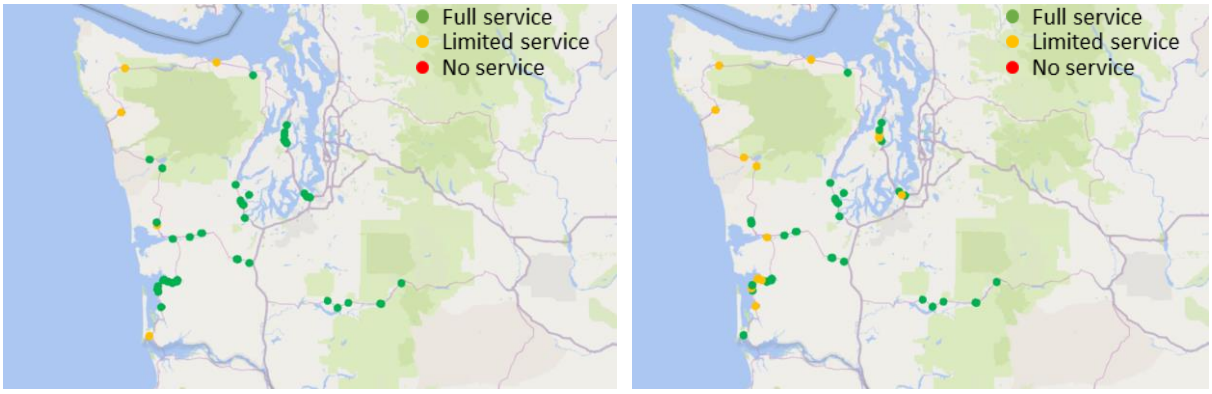

Figure 4.5. Predicted bridge functionality maps for median ductility demand results. Left: Fixed-fixed boundary condition period assumption, Right: fixed-pin boundary condition period assumption

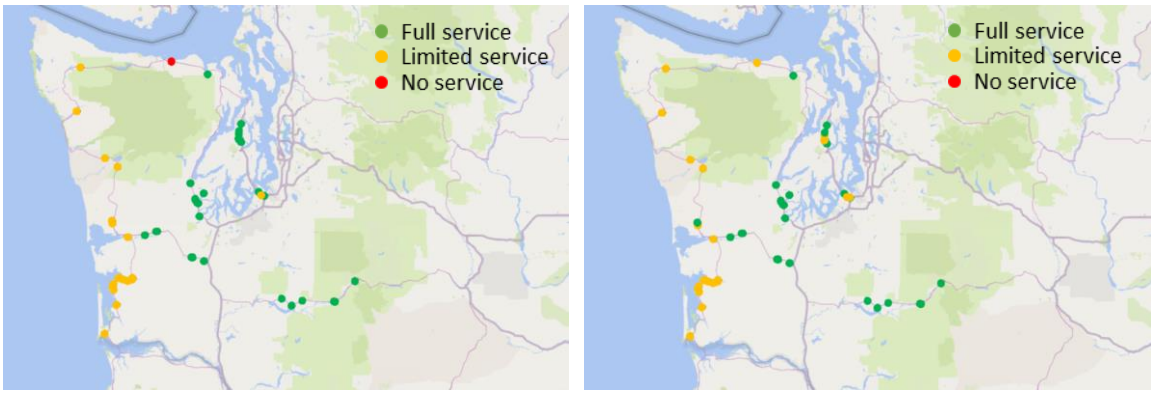

Figure 4.6. Predicted bridge functionality maps for 84th percentile ductility demand results. Left: Fixed-fixed boundary condition period assumption, Right: fixed-pin boundary condition period assumption

The functionality maps shown in figure 4.5 and figure 4.6 are not without limitations. The most significant limitations were the use of site class C soil conditions for all analyses and exclusion of non-ductile responses, such as shear failure and foundation failure. Site class C soil is relatively stiff and not prone to liquefaction. As shown by Kortum et al. (2021), softer soil profiles, such as site class D, would further amplify seismic forces, increasing the ductility

demand. Additionally, some sites around Washington state are prone to the occurrence of liquefaction, which could result in significant bridge damage.

Despite the limitations of the analyses, the results suggested a significantly different post-earthquake serviceability of the Washington bridge network than reported by the DHS RRAP report. This is evident from figure 4.7, which shows the map of predicted reopening times of the full Washington bridge network from the RRAP report and the worst case functionality map from this project, which was based on 84th percentile response curves and fixed-fixed column boundary conditions. The Washington BDM says that limited service bridges are expected to be repairable to reduced volume service within three months of an earthquake. This project did not consider every bridge in Washington and differed from the RRAP report in this regard. As shown by figure 4.7, while repairs would likely be necessary along the coast, and the number of repairs could slow the re-opening schedule, the likelihood of widespread significant bridge damage would be relatively low. Therefore, the emergency management plan of Western Washington can likely rely on ground transportation modes to transport resources and people across the state or to the I-5/405/90 lifeline corridors.

< 1 week or undamaged
1-3 months
> 1 year, replacement needed

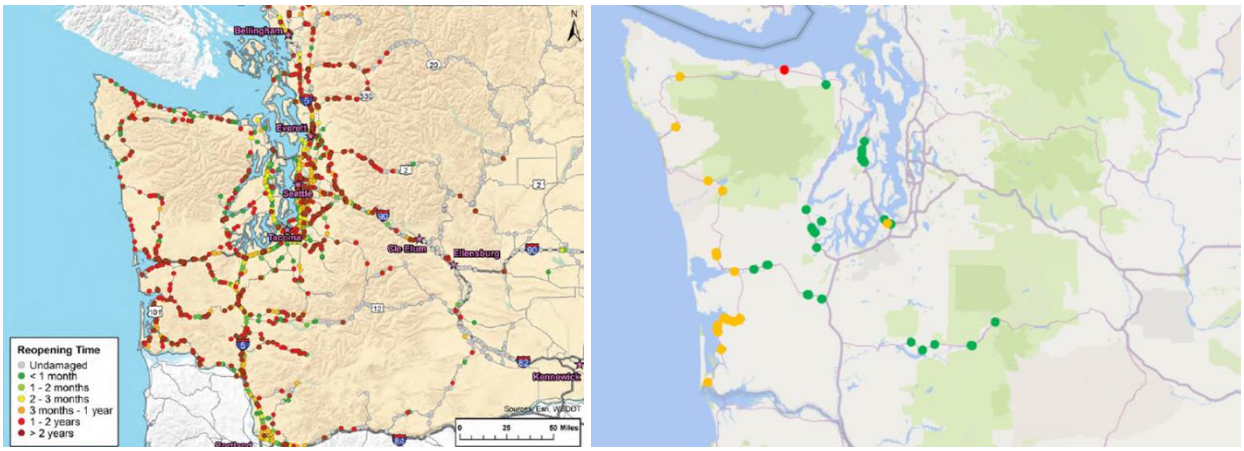

Figure 4.7. Comparison of RRAP report reopening time predictions (left) and analysis results from this project (right).

Fragility plots for each bridge location and period showing the probability of exceeding any displacement ductility between 0 and 8 are provided in figure 4.8 and figure 4.9 for periods of 0.2 and 1.0 seconds, respectively. Plots for all periods analyzed are included in Appendix A. These plots can be used to assist in evaluation of specific bridges based on period and location. To determine the likelihood of a bridge exceeding a certain ductility demand, an evaluator could use the plots that bound the bridge period to interpolate the probability of exceedance for any of the ten sites analyzed. As shown by the figures, there is more variation in predicted ductility demand across the ten locations for the longer period bridges than for the shorter period bridges because of sedimentary basin effects.

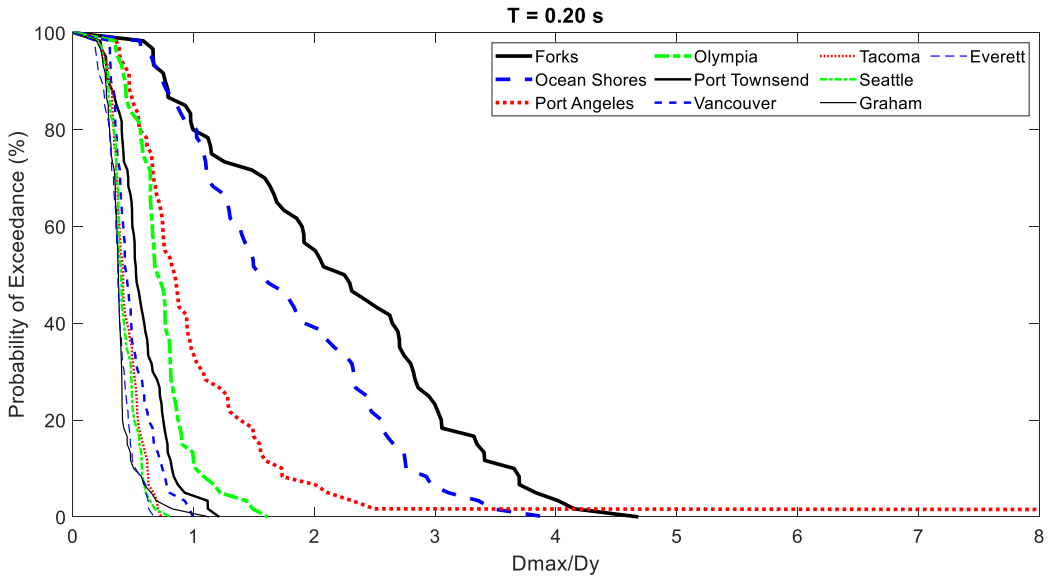

Figure 4.8. Example displacement ductility fragility for 0.20-second period bridges

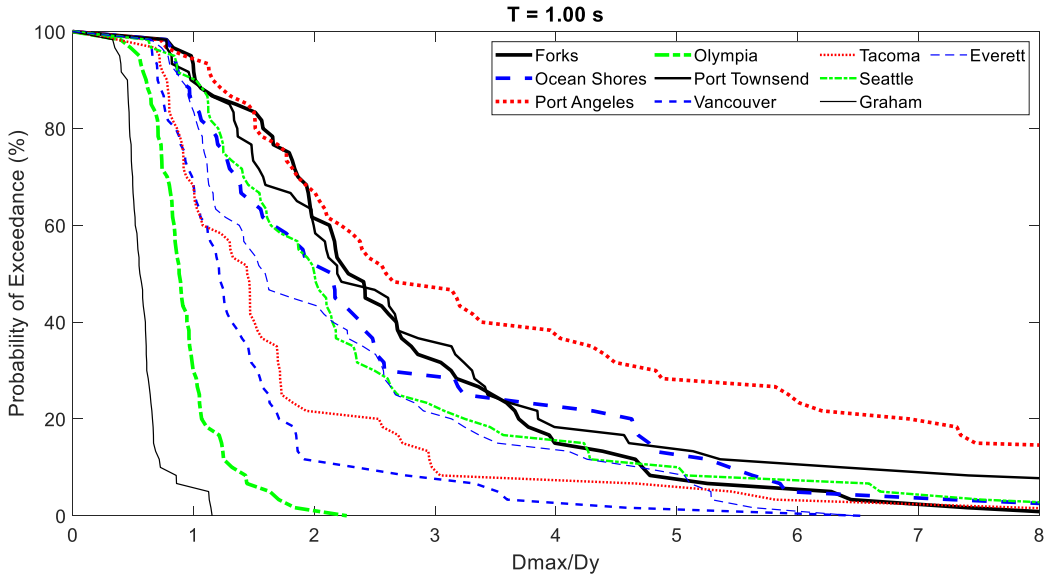

Figure 4.9. Example displacement ductility fragility for 1.00-second period bridges

CHAPTER 5. CONCLUSIONS

In this project, the WSDOT bridge database was expanded to add the properties of 58 additional bridges located on secondary routes that feed into the I-5/405/90 lifeline corridors. The additional bridge properties were used to define the parameters for a parametric study investigating the effects of an M9 Cascadia Subduction Zone earthquake on bridge functionality in Western Washington. From the WSDOT bridge database, 21 single degree-of-freedom models were calibrated to experimental tests of reinforced concrete columns by using a procedure described by Kortum et al. (2021). The models were analyzed for 30 scenarios of CSZ earthquakes at ten locations across Western Washington. Results from the model analyses were used to provide a more detailed understanding of the likelihood of bridge damage on the secondary routes feeding into the WSDOT lifeline routes and the likely service levels post-earthquake. Several conclusions were made that WSDOT and Washington state emergency planning officials can use to better prepare for a possible M9 CSZ earthquake:

- The secondary route bridges are largely similar in characteristics to the lifeline route bridges, with the exception that secondary route bridges are generally smaller and, therefore, have smaller average column diameters of 10 to 20 inches in comparison to 30 to 40 inches. Bridge construction years, configurations, periods, and numbers of spans are all similar. Only one secondary route bridge added to the database had been seismically retrofitted with steel jackets.
- In comparison to the conclusions of the DHS RRAP report, post-earthquake bridge functionality would likely be considerably better than anticipated, with most bridges along the coast likely to need repair but still useable for emergency vehicles and post-earthquake response.

- Most bridges located inland and outside of the basin were predicted to be capable of full service post-earthquake. This means routes across the Cascade mountains should be fully open.
- For inland regions within sedimentary basins, such as Seattle, bridges with periods of between 1.0 and 3.0 seconds would likely sustain moderate damage, resulting in limited service. Short period bridges in these regions would likely be able to retain full service.
- Port Angeles, Forks, and Ocean Shores are the regions of Western Washington with the highest probability of significant bridge damage. At these locations, the probability of exceeding a displacement ductility demand of 2.0, which is the limit for minor damage and, therefore, little-to-no repair, was found to be greater than 40 percent for most periods of less than 3.0 seconds.
- The likelihood of significant damage, collapse, or total loss of service post-earthquake was found to be below 20 percent for all regions of Western Washington, except Port Angeles.

REFERENCES

Chandramohan, R., Baker, J., and Deierlein, G. (2019). "Quantifying the Influence of Ground Motion Duration on Structural Collapse Capacity Using Spectrally Equivalent Records". *Earthquake Spectra*, 32(2): 927-950.

De Zamacona Cervantes, G. (2019). "Response of Idealized Structural Systems to Simulated M9 Cascadia Subduction Zone Earthquakes Considering Local Soil Conditions." Master's Thesis, University of Washington, Seattle, WA.

DHS, 2019. *Regional Resiliency Assessment Program (RRAP): Resiliency Assessment of Washington State Transportation Systems*, Washington, D.C.: Department of Homeland Security.

Elwood, K. and Eberhard, M. (2009). "Effective Stiffness of Reinforced Concrete Columns," *ACI Structural Journal*, July-August Issue: 476-484.

Frankel, A., E. Wirth, N. Marafi, J. Vidale, and W. Stephenson. (2018). Broadband Synthetic Seismograms for Magnitude 9 Earthquakes on the Cascadia Megathrust Based on 3D Simulations and Stochastic Synthetics, Part 1: Methodology and Overall Results. *Bulletin of the Seismological Society of America*; 108(5A): 2347–2369. doi: https://doi.org/10.1785/0120180034.

Gidaris, I., Padgett, J. E., Barbosa, A. R. & Chen, S., 2017. Multiple-Hazard Fragility and Restoration Models of Highway Bridges for Regional Risk and Resilience Assessment in the United States: State of the Art Review. *Journal of Structural Engineering*, 3(143).

Haselton, C., Liel, A., Lange, S., and Deierlein, G. (2008). "Beam-Column Element Model Calibrated for Predicting Flexural Response Leading to Global Collapse of RC Frame Buildings." *PEER Report 2007/03*.

Kortum, Z., Liu, K.J., Eberhard, M., Berman, J., Marafi, N., and Maurer, B. (2021). "Impacts of Cascadia Subduction Zone M9 Earthquakes on Bridges in Washington State: SDOF Idealized Bridges." *WSDOT Final Report T1461, Task 74.* (Forthcoming).

Lignos, D.G. and Krawinkler, H. (2012). "Sidesway collapse of deteriorating structural systems under seismic excitations," *Rep.No.TB 177*, The John A. Blume Earthquake Engineering Research Center, Stanford University, Stanford, CA.

Marafi, N.A., Eberhard, M.O., Berman, J.W., Wirth, E.A., and Frankel, A.D. (2017). "Effects of Deep Basins on Structural Collapse During Large Subduction Zone Earthquakes." *Earthquake Spectra*, 33(3), 963-997. https://doi.org/10.1193/071916EQS114M

Marafi, N., Makdisi, A., Eberhard, M., and Berman, J. (2020). "Performance of RC Core-Wall Buildings during Simulated M9 Cascadia Subduction Zone Earthquake Scenarios". *Journal of Structural Engineering*, 146(2).

Pacific Northwest Seismic Network. (2021). “Cascadia Subduction Zone.” https://pnsn.org/outreach/ earthquakesources/csz (May 31, 2021).

Ranf, R. T., Eberhard, M. & Malone, S., (2007). Post-Earthquake Prioritization of Bridge Inspections. *Earthquake Spectra*, Issue February, pp. 131-146.

WSDOT. (2020). *Bridge Design Manual M 23-50.20.* Washington State Department of Transportation, Bridge and Structures Office.

APPENDIX A

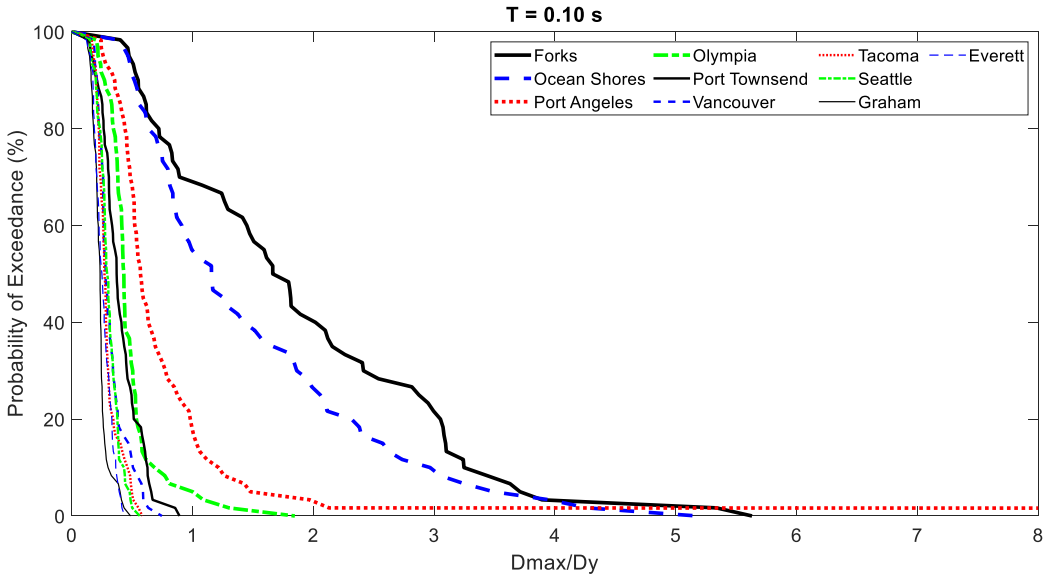
T = 0.10 s
Forks
Olympia
Tacoma
Everett
Ocean Shores
Port Townsend
Seattle
Port Angeles
Vancouver
Graham
Probability of Exceedance (%)
Dmax/Dy
0
20
40
60
80
100
0
1
2
3
4
5
6
7
8

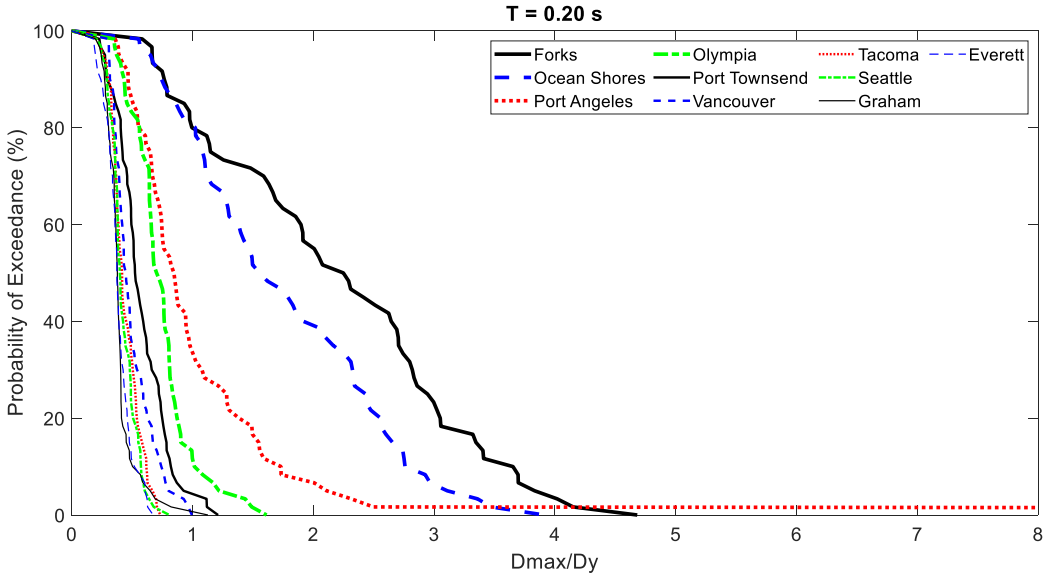
T = 0.20 s
Forks
Olympia
Tacoma
Everett
Ocean Shores
Port Townsend
Seattle
Port Angeles
Vancouver
Graham
Probability of Exceedance (%)
Dmax/Dy
0
20
40
60
80
100
0
1
2
3
4
5
6
7
8

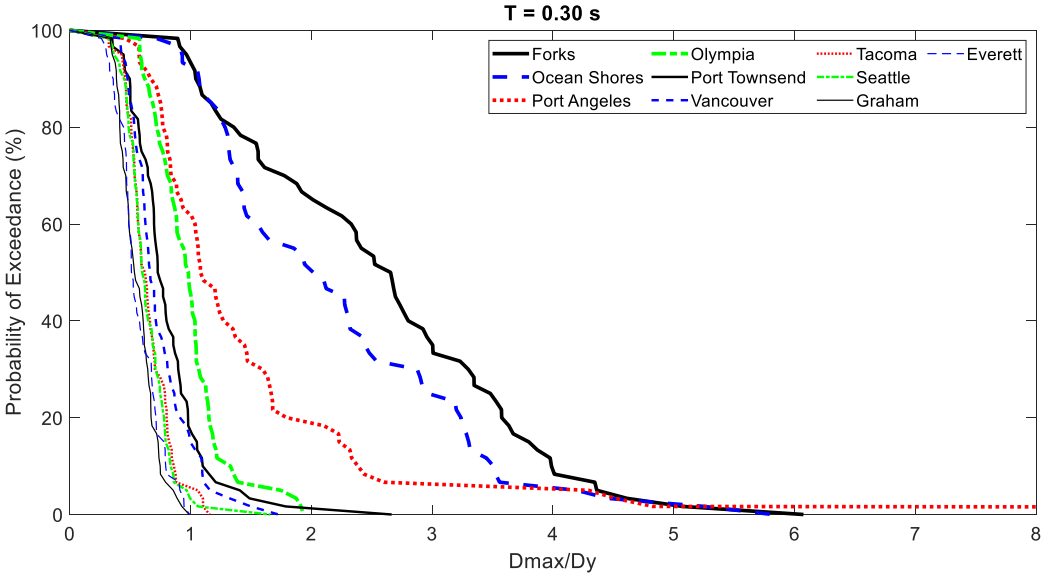
T = 0.30 s
Forks
Olympia
Tacoma
Everett
Ocean Shores
Port Townsend
Seattle
Port Angeles
Vancouver
Graham
Probability of Exceedance (%)
Dmax/Dy
0
20
40
60
80
100
0
1
2
3
4
5
6
7
8

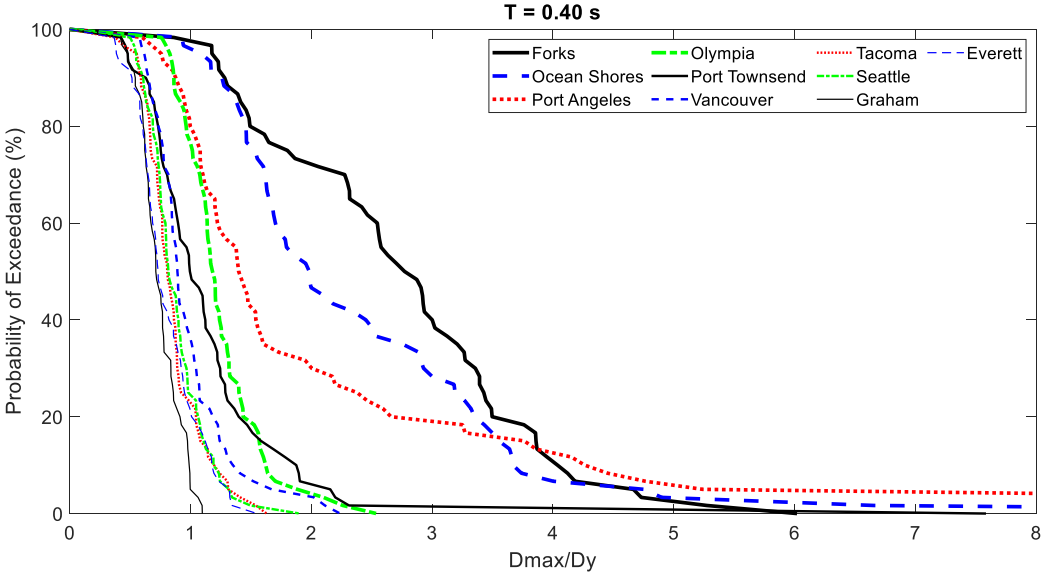
T = 0.40 s
Forks
Olympia
Tacoma
Everett
Ocean Shores
Port Townsend
Seattle
Port Angeles
Vancouver
Graham
Probability of Exceedance (%)
Dmax/Dy
0
20
40
60
80
100
0
1
2
3
4
5
6
7
8

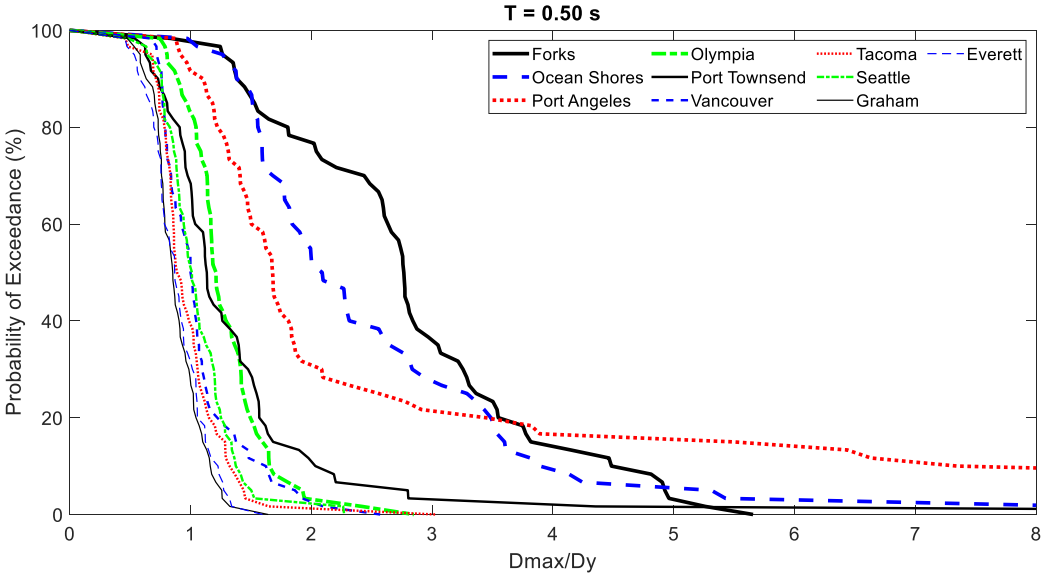
T = 0.50 s
Forks
Olympia
Tacoma
Everett
Ocean Shores
Port Townsend
Seattle
Port Angeles
Vancouver
Graham
Probability of Exceedance (%)
Dmax/Dy
0
20
40
60
80
100
0
1
2
3
4
5
6
7
8

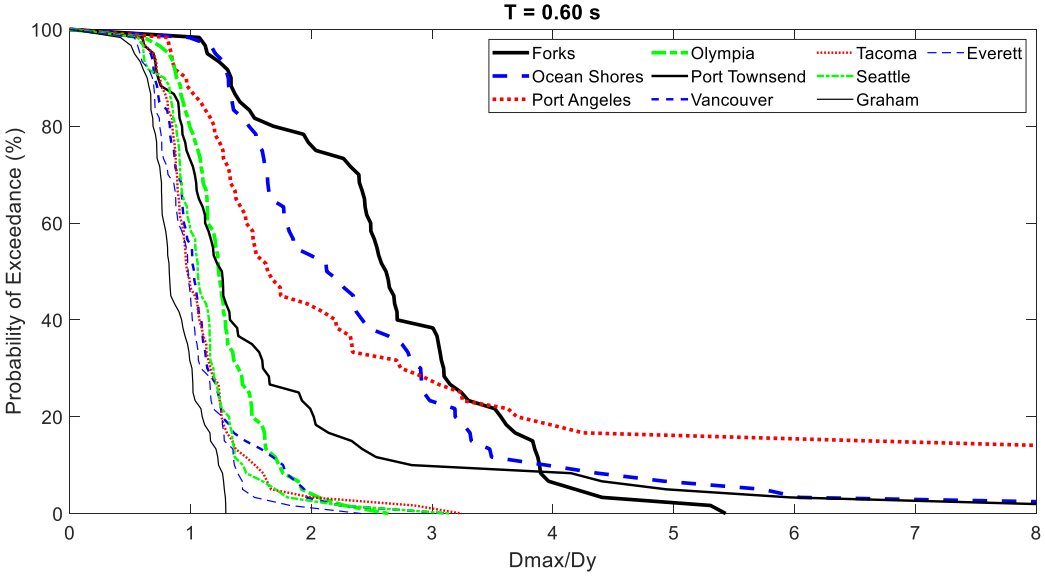
T = 0.60 s
Forks
Olympia
Tacoma
Everett
Ocean Shores
Port Townsend
Seattle
Port Angeles
Vancouver
Graham
Probability of Exceedance (%)
Dmax/Dy
0
20
40
60
80
100
0
1
2
3
4
5
6
7
8

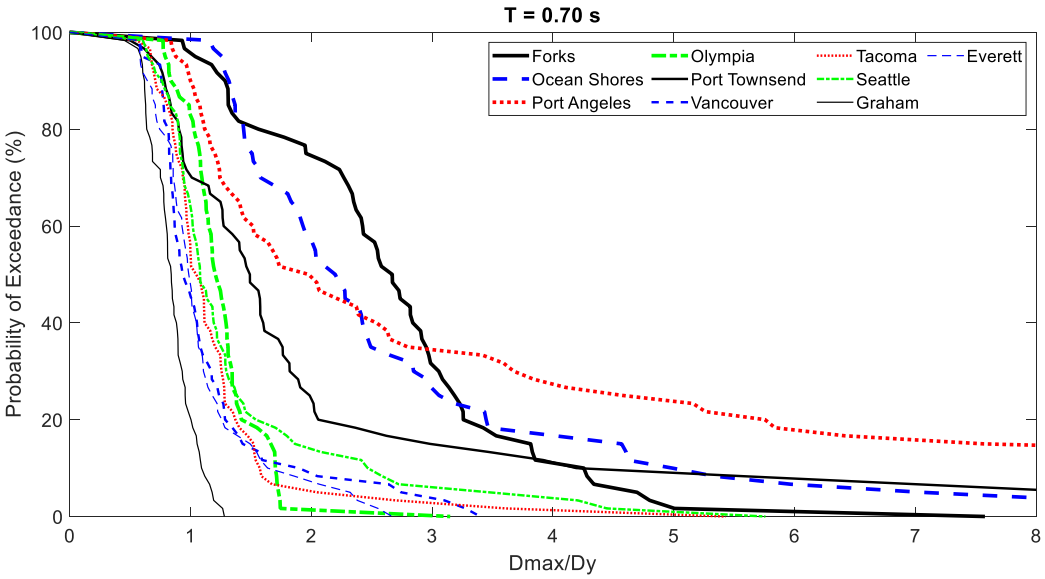
T = 0.70 s
Forks
Olympia
Tacoma
Everett
Ocean Shores
Port Townsend
Seattle
Port Angeles
Vancouver
Graham
Probability of Exceedance (%)
Dmax/Dy
0
20
40
60
80
100
0
1
2
3
4
5
6
7
8

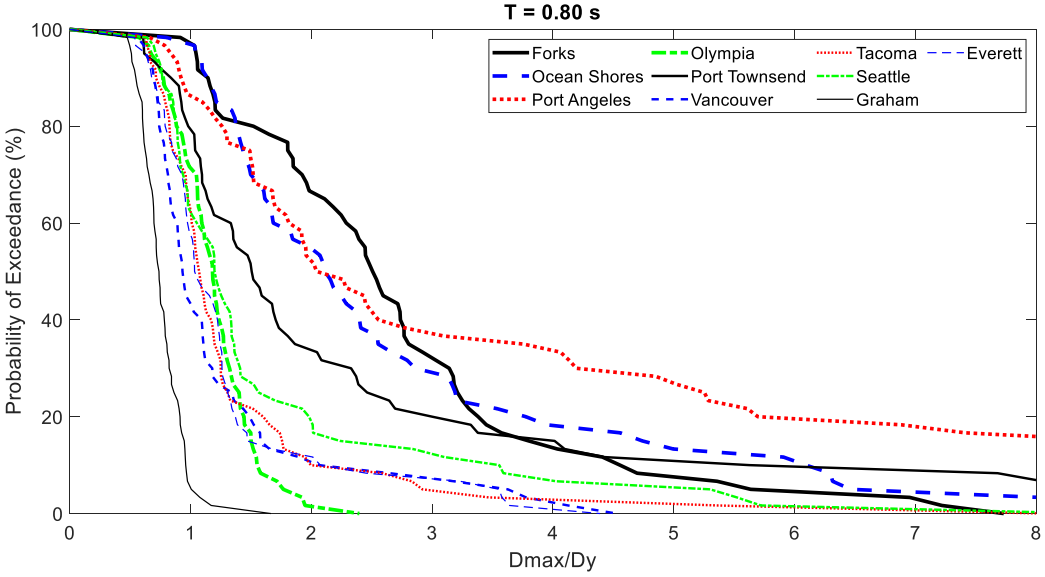
T = 0.80 s
Forks
Olympia
Tacoma
Everett
Ocean Shores
Port Townsend
Seattle
Port Angeles
Vancouver
Graham
Probability of Exceedance (%)
Dmax/Dy
0
20
40
60
80
100
0
1
2
3
4
5
6
7
8

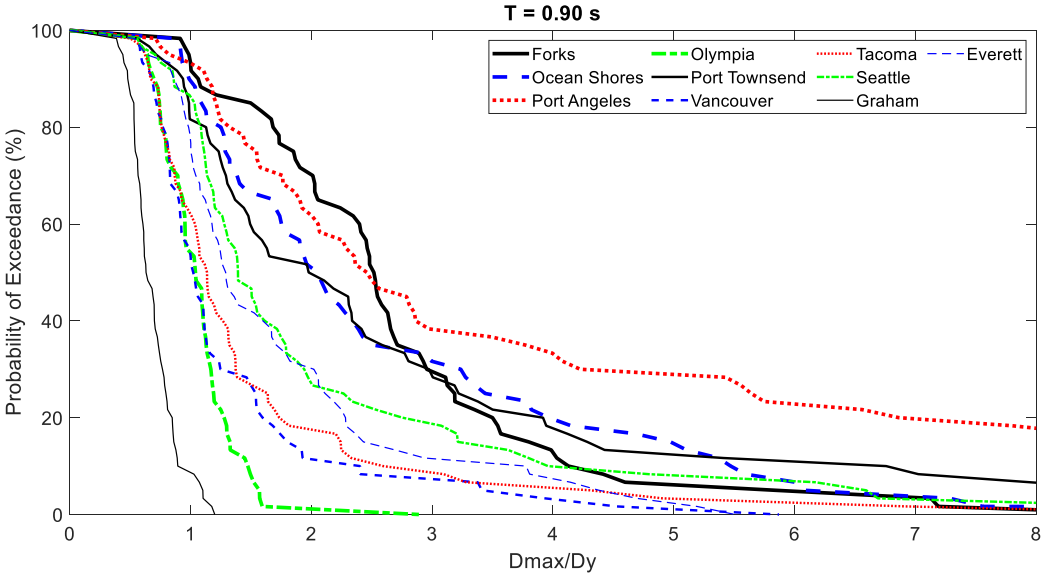
T = 0.90 s
Forks
Olympia
Tacoma
Everett
Ocean Shores
Port Townsend
Seattle
Port Angeles
Vancouver
Graham
Probability of Exceedance (%)
Dmax/Dy
0
20
40
60
80
100
0
1
2
3
4
5
6
7
8

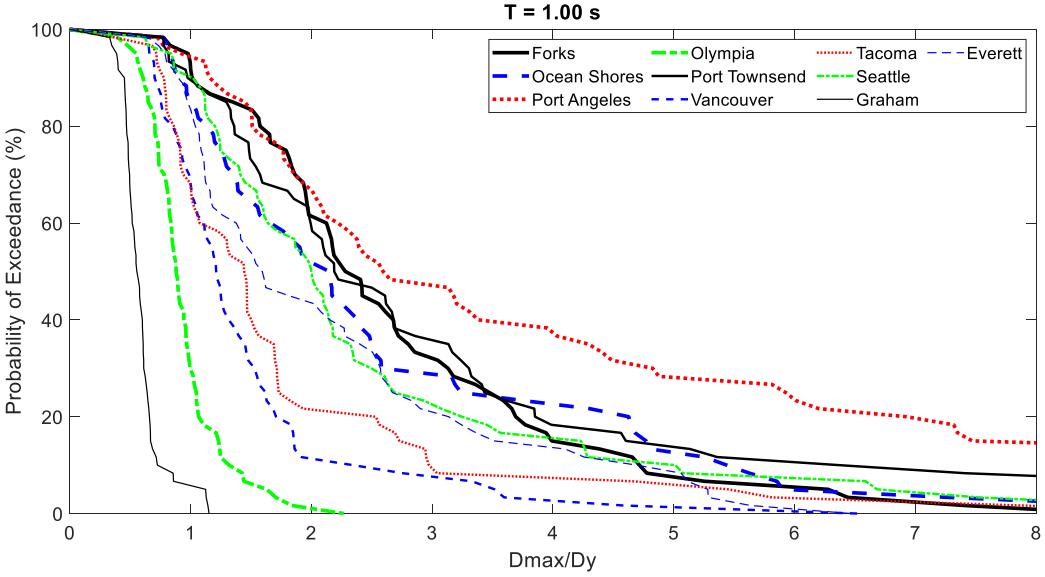
T = 1.00 s
Forks
Olympia
Tacoma
Everett
Ocean Shores
Port Townsend
Seattle
Port Angeles
Vancouver
Graham
Probability of Exceedance (%)
Dmax/Dy
0
20
40
60
80
100
0
1
2
3
4
5
6
7
8

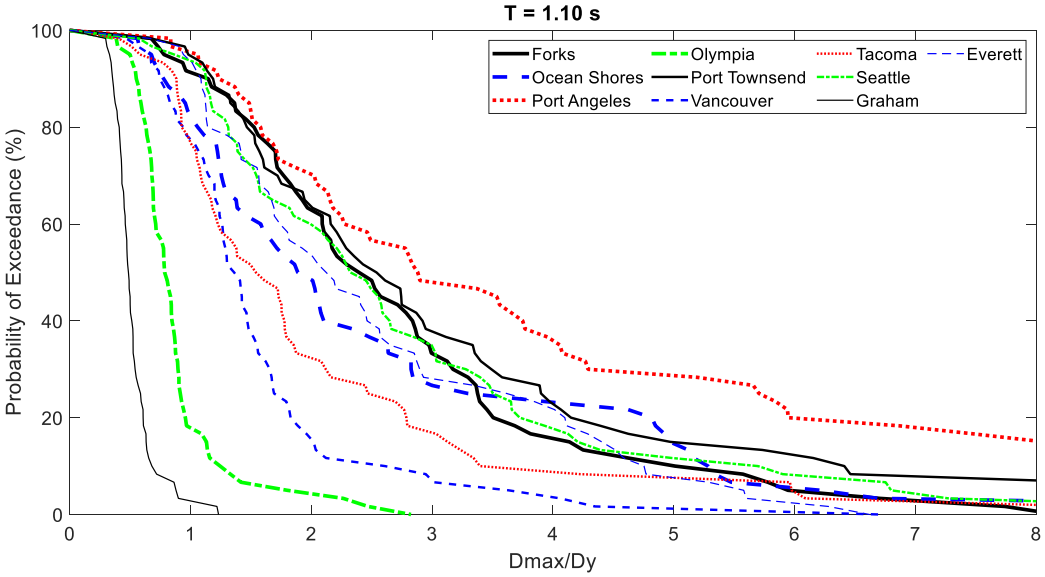
T = 1.10 s
Forks
Olympia
Tacoma
Everett
Ocean Shores
Port Townsend
Seattle
Port Angeles
Vancouver
Graham
Probability of Exceedance (%)
Dmax/Dy
0
20
40
60
80
100
0
1
2
3
4
5
6
7
8

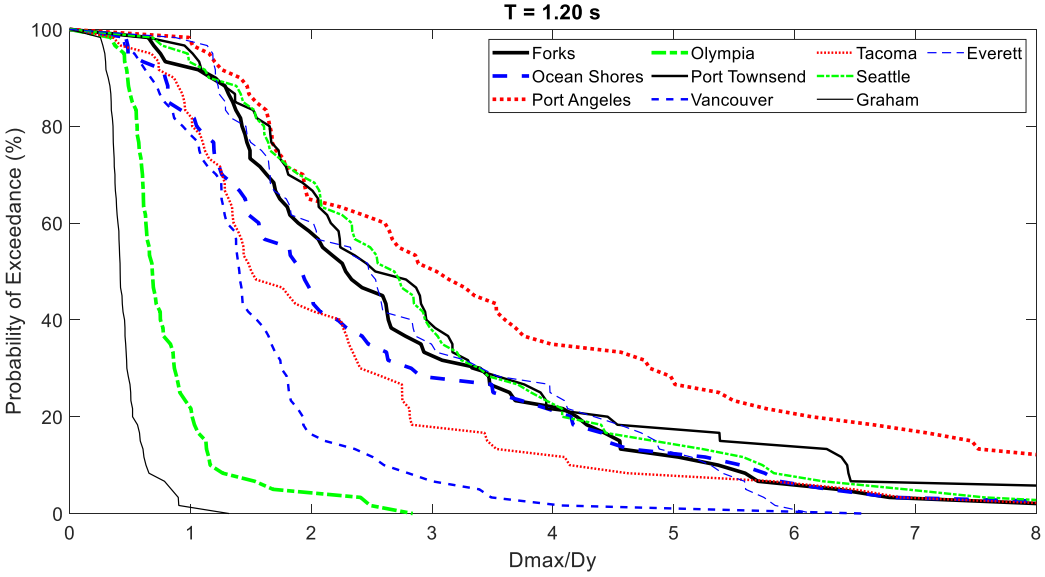
T = 1.20 s
Forks
Olympia
Tacoma
Everett
Ocean Shores
Port Townsend
Seattle
Port Angeles
Vancouver
Graham
Probability of Exceedance (%)
Dmax/Dy
0
20
40
60
80
100
0
1
2
3
4
5
6
7
8

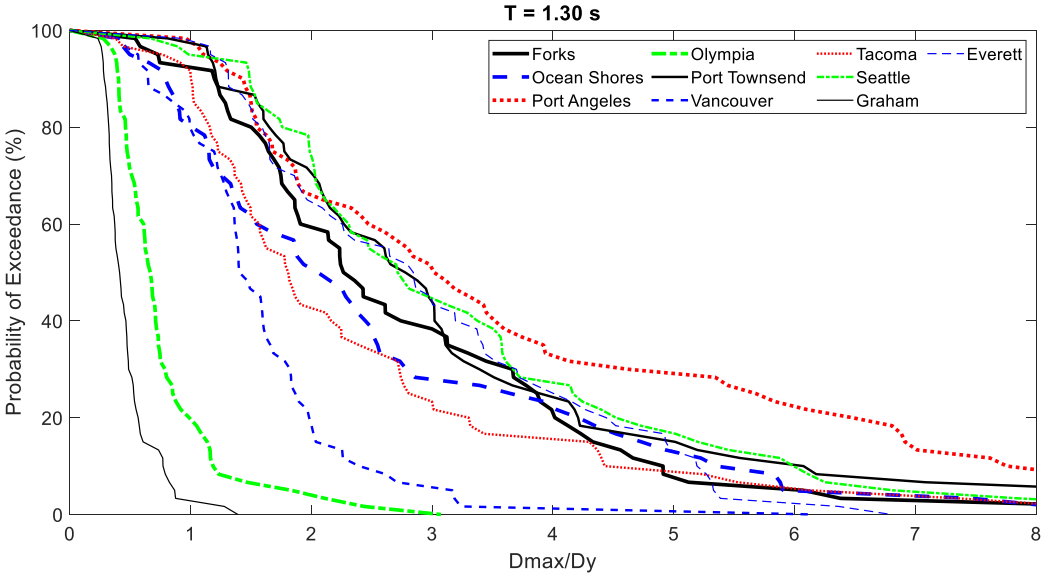
T = 1.30 s
Forks
Olympia
Tacoma
Everett
Ocean Shores
Port Townsend
Seattle
Port Angeles
Vancouver
Graham
Probability of Exceedance (%)
Dmax/Dy
0
20
40
60
80
100
0
1
2
3
4
5
6
7
8

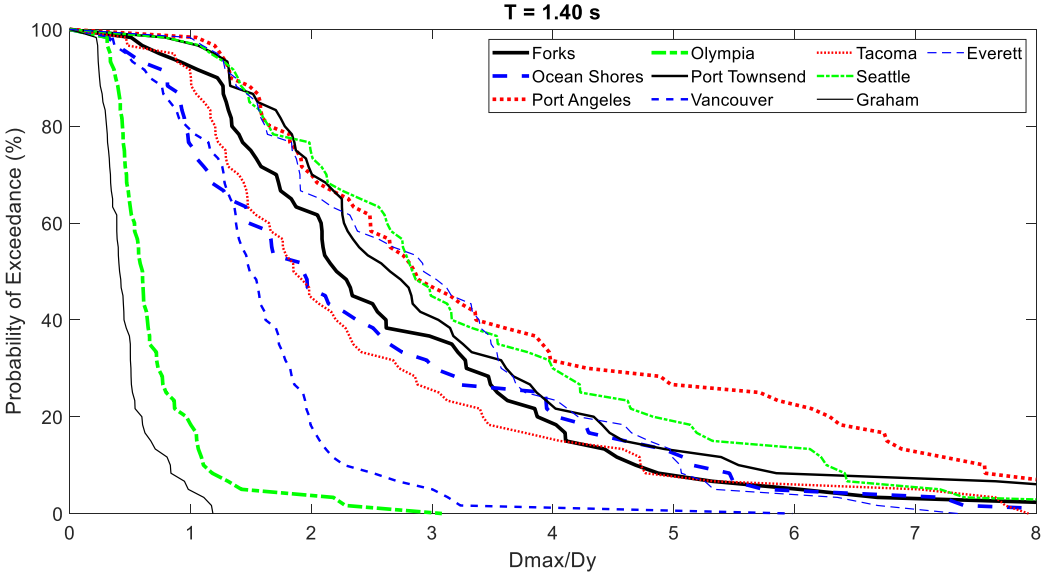
T = 1.40 s
Forks
Olympia
Tacoma
Everett
Ocean Shores
Port Townsend
Seattle
Port Angeles
Vancouver
Graham
Probability of Exceedance (%)
Dmax/Dy
0
20
40
60
80
100
0
1
2
3
4
5
6
7
8

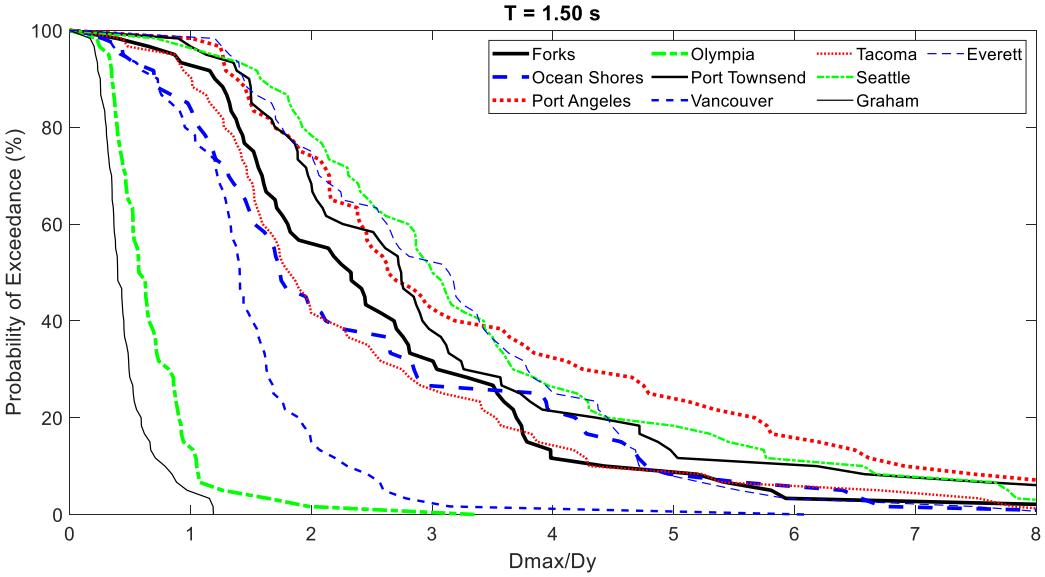
T = 1.50 s
Probability of Exceedance (%)
Dmax/Dy
Forks
Olympia
Tacoma
Everett
Ocean Shores
Port Townsend
Seattle
Port Angeles
Vancouver
Graham

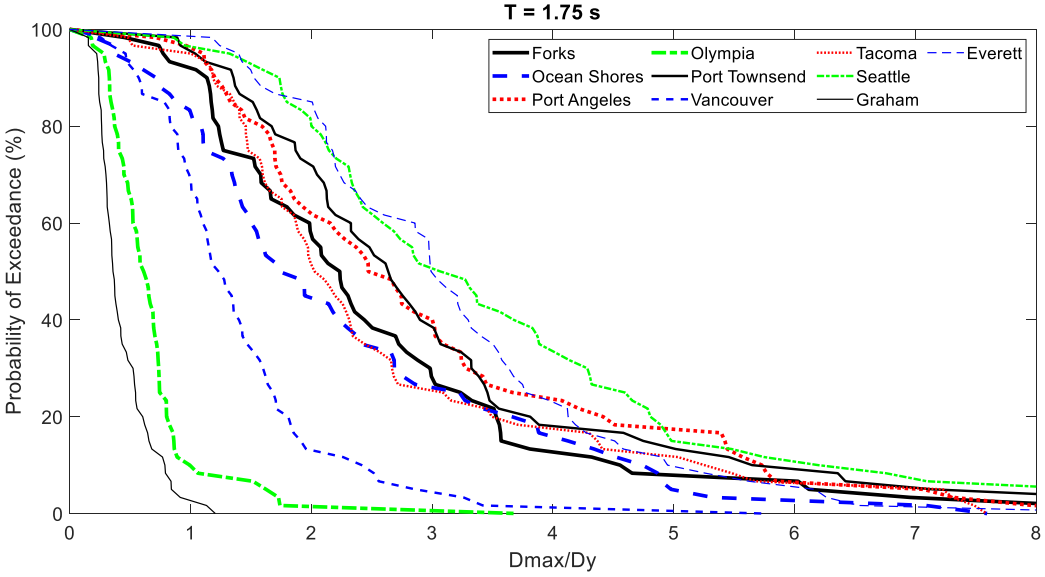
T = 1.75 s
Probability of Exceedance (%)
Dmax/Dy
Forks
Olympia
Tacoma
Everett
Ocean Shores
Port Townsend
Seattle
Port Angeles
Vancouver
Graham

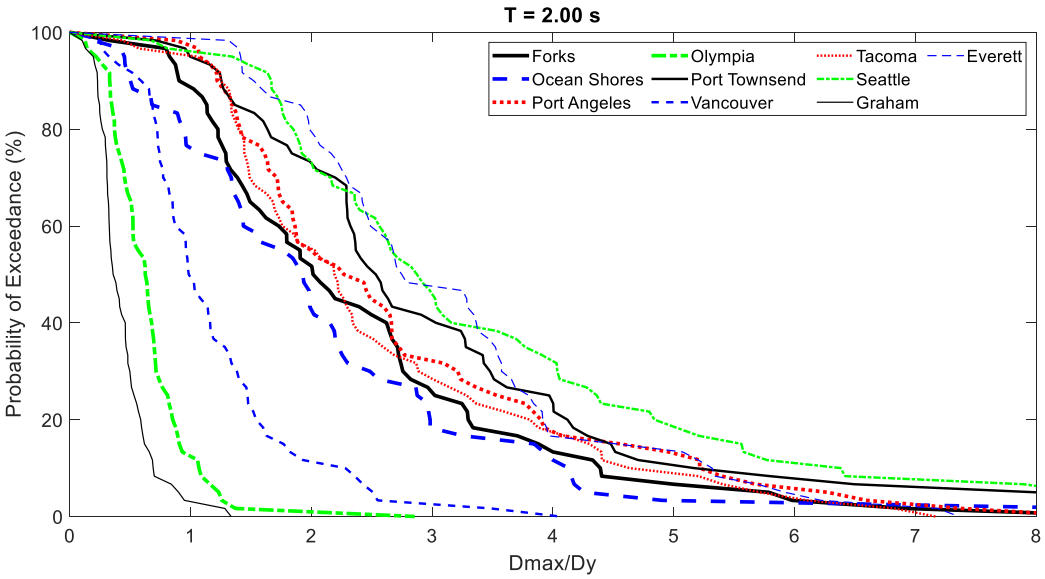
T = 2.00 s
Forks
Olympia
Tacoma
Everett
Ocean Shores
Port Townsend
Seattle
Port Angeles
Vancouver
Graham
Probability of Exceedance (%)
Dmax/Dy
0
20
40
60
80
100
0
1
2
3
4
5
6
7
8

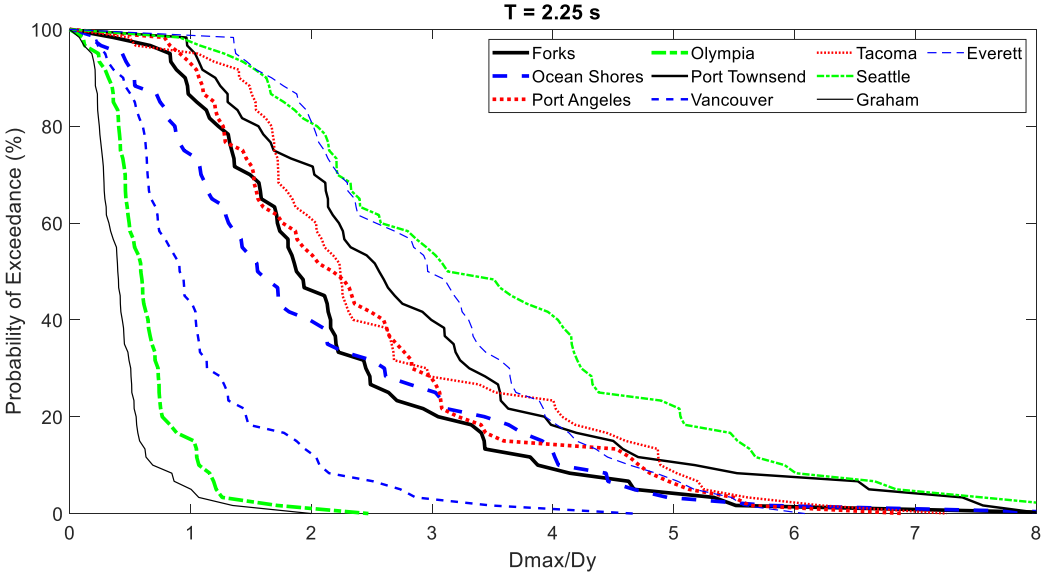
T = 2.25 s
Forks
Olympia
Tacoma
Everett
Ocean Shores
Port Townsend
Seattle
Port Angeles
Vancouver
Graham
Probability of Exceedance (%)
Dmax/Dy
0
20
40
60
80
100
0
1
2
3
4
5
6
7
8

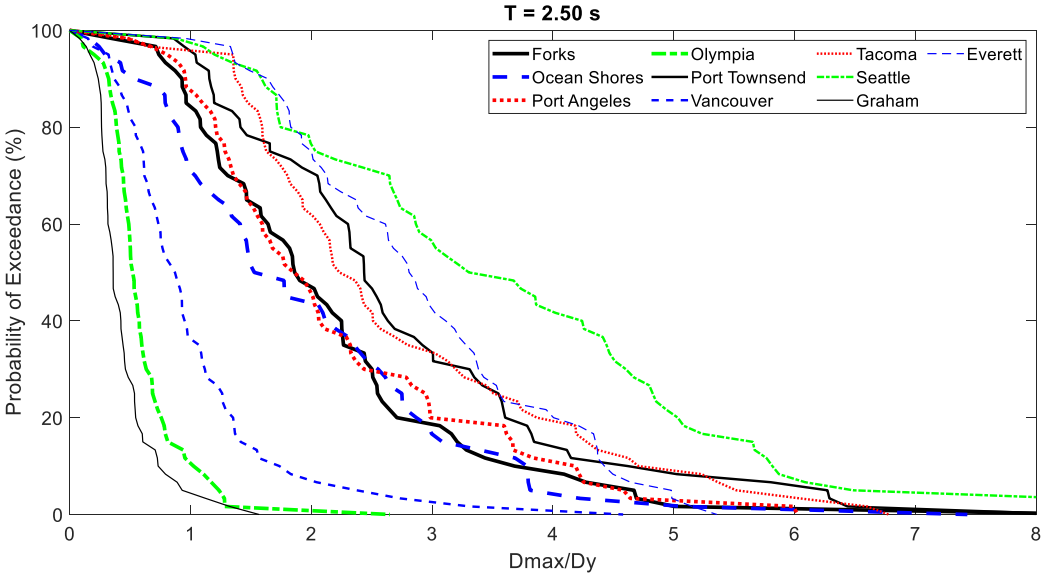
T = 2.50 s
Forks
Olympia
Tacoma
Everett
Ocean Shores
Port Townsend
Seattle
Port Angeles
Vancouver
Graham
Probability of Exceedance (%)
Dmax/Dy
0
20
40
60
80
100
0
1
2
3
4
5
6
7
8

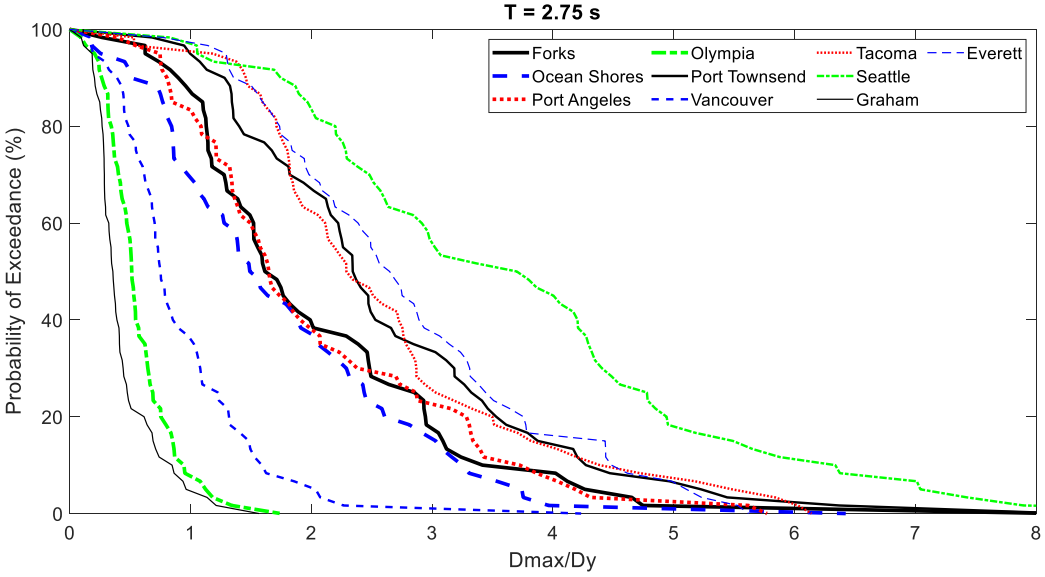
T = 2.75 s
Forks
Olympia
Tacoma
Everett
Ocean Shores
Port Townsend
Seattle
Port Angeles
Vancouver
Graham
Probability of Exceedance (%)
Dmax/Dy
0
20
40
60
80
100
0
1
2
3
4
5
6
7
8

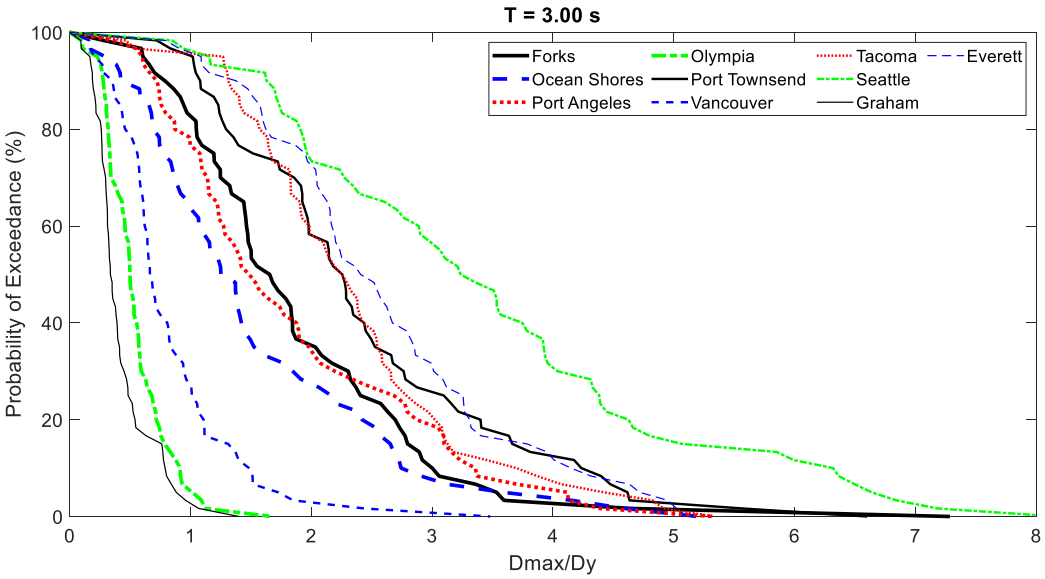
T = 3.00 s
Forks
Olympia
Tacoma
Everett
Ocean Shores
Port Townsend
Seattle
Port Angeles
Vancouver
Graham
Probability of Exceedance (%)
Dmax/Dy
0
20
40
60
80
100
0
1
2
3
4
5
6
7
8

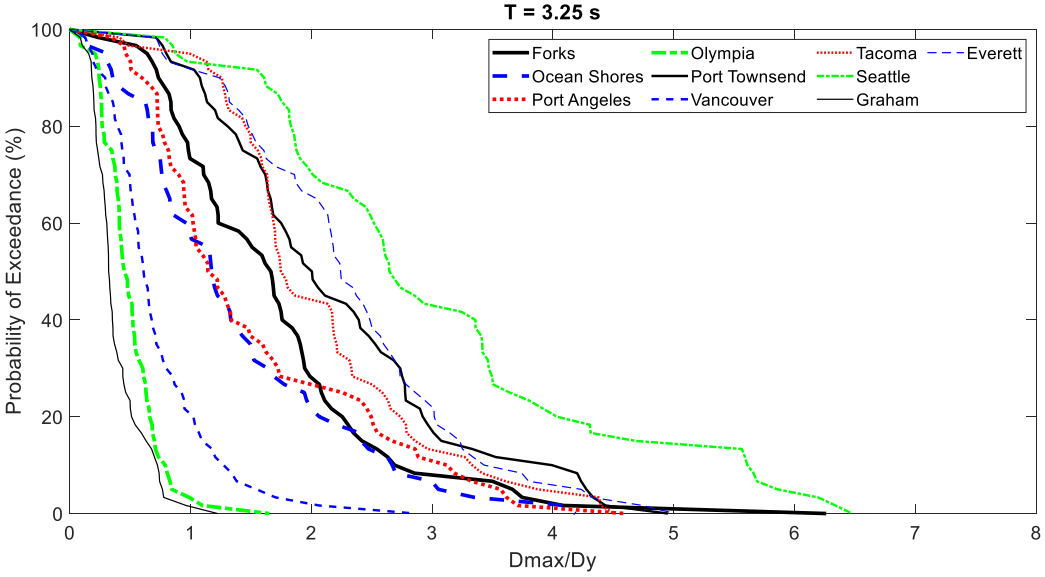
T = 3.25 s
Forks
Olympia
Tacoma
Everett
Ocean Shores
Port Townsend
Seattle
Port Angeles
Vancouver
Graham
Probability of Exceedance (%)
Dmax/Dy
0
20
40
60
80
100
0
1
2
3
4
5
6
7
8

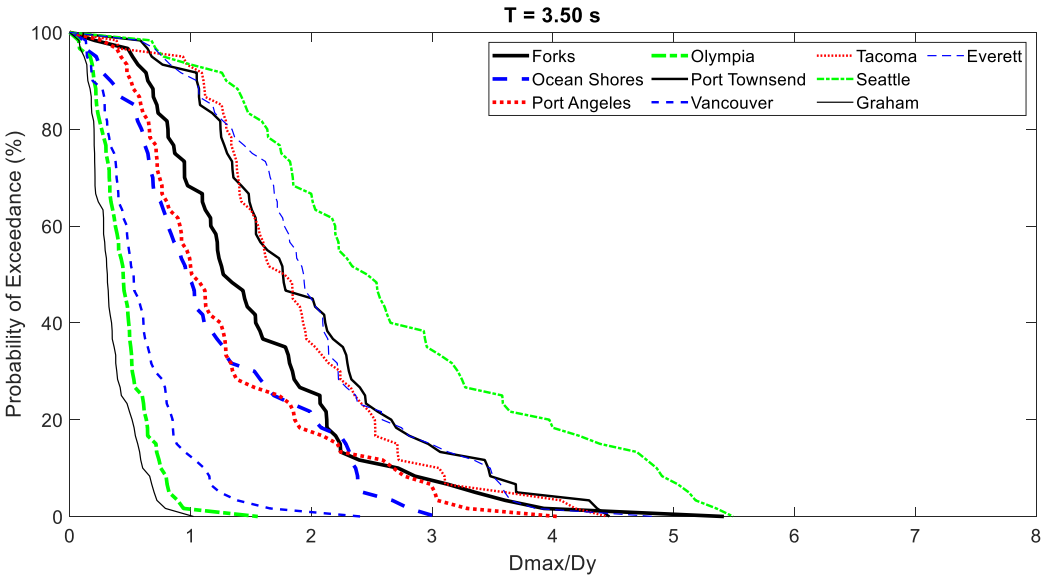
T = 3.50 s
Forks
Olympia
Tacoma
Everett
Ocean Shores
Port Townsend
Seattle
Port Angeles
Vancouver
Graham
Probability of Exceedance (%)
Dmax/Dy
0
20
40
60
80
100
0
1
2
3
4
5
6
7
8

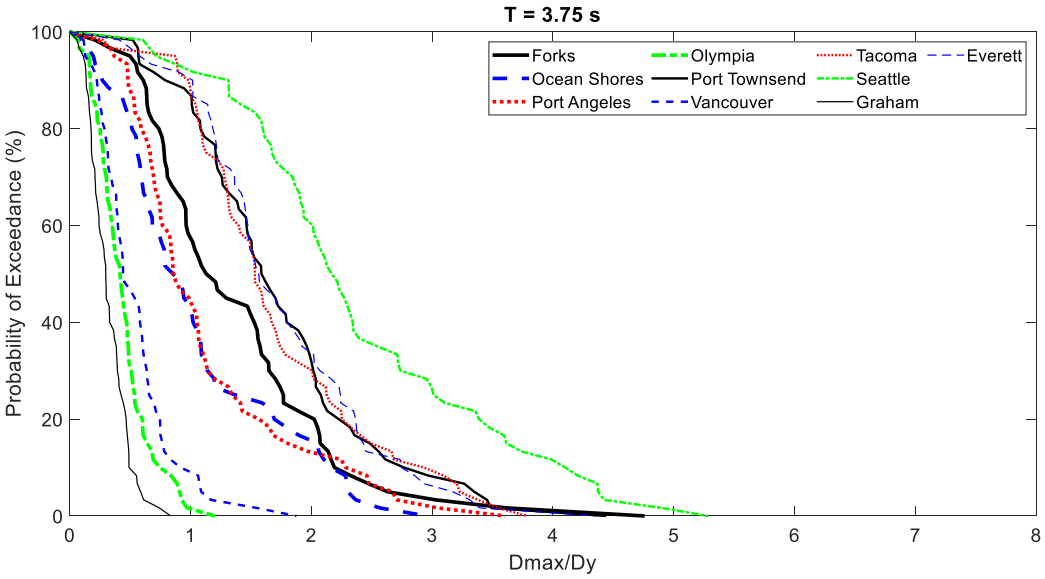
T = 3.75 s
Forks
Olympia
Tacoma
Everett
Ocean Shores
Port Townsend
Seattle
Port Angeles
Vancouver
Graham
Probability of Exceedance (%)
Dmax/Dy
0
20
40
60
80
100
0
1
2
3
4
5
6
7
8

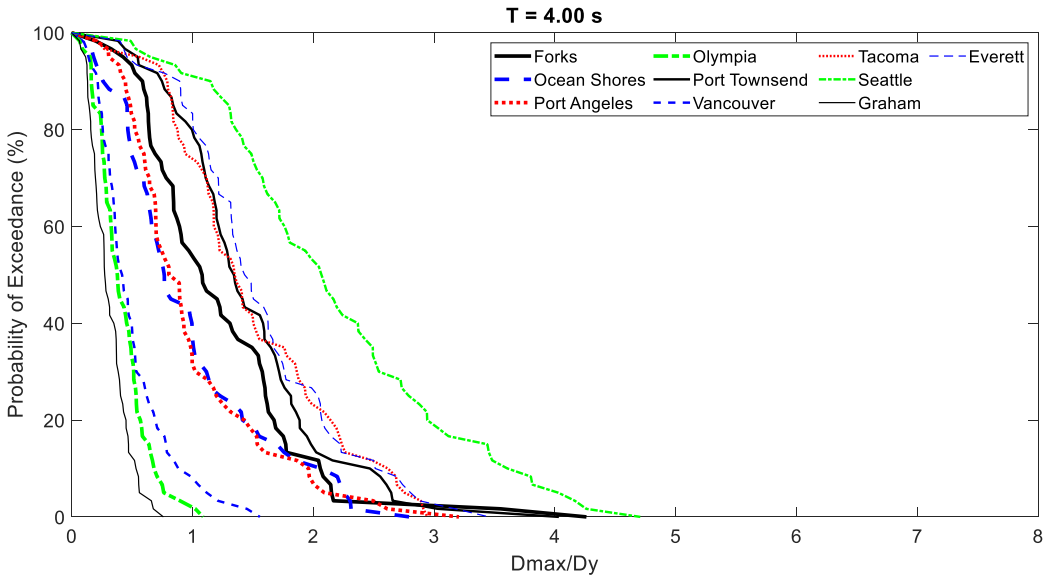
T = 4.00 s
Forks
Olympia
Tacoma
Everett
Ocean Shores
Port Townsend
Seattle
Port Angeles
Vancouver
Graham
Probability of Exceedance (%)
Dmax/Dy
0
20
40
60
80
100
0
1
2
3
4
5
6
7
8